Received: 10 August 2021 | Accepted: 1 September 2021

DOI: 10.1111/mmi.14807

RESEARCH ARTICLE

WILEY

PIP5KIγ90-generated phosphatidylinositol-4,5-bisphosphate promotes the uptake of *Staphylococcus aureus* by host cells

Yong Shi[1] | Anne Berking[1] | Timo Baade[1,2] | Kyle R. Legate[3] | Reinhard Fässler[3] | Christof R. Hauck[1,2]

[1]Lehrstuhl für Zellbiologie, Universität Konstanz, Konstanz, Germany

[2]Konstanz Research School Chemical Biology, Universität Konstanz, Konstanz, Germany

[3]MPI for Biochemistry, Martinsried, Germany

Correspondence
Christof R. Hauck, Lehrstuhl für Zellbiologie, Universität Konstanz, Universitätsstraße 10, Postablage 621, 78457 Konstanz, Germany.
Email: christof.hauck@uni-konstanz.de

Present address
Anne Berking, Berking Biotechnology SpA, Avenida Torobayo 2102, Valdivia, 511-0566, Chile

Funding information
Deutsche Forschungsgemeinschaft, Grant/Award Number: Ha 2856/5-1; Chinese Scholarship Council

Abstract

Staphylococcus aureus, a Gram-positive pathogen, invades cells mainly in an integrin-dependent manner. As the activity or conformation of several integrin-associated proteins can be regulated by phosphatidylinositol-4,5-bisphosphate (PI-4,5-P_2), we investigated the roles of PI-4,5-P_2 and PI-4,5-P_2-producing enzymes in cellular invasion by *S. aureus*. PI-4,5-P_2 accumulated upon contact of *S. aureus* with the host cell, and targeting of an active PI-4,5-P_2 phosphatase to the plasma membrane reduced bacterial invasion. Knockdown of individual phosphatidylinositol-4-phosphate 5-kinases revealed that phosphatidylinositol-4-phosphate 5-kinase γ (PIP5KIγ) plays an important role in bacterial internalization. Specific ablation of the talin and FAK-binding motif in PIP5KIγ90 reduced bacterial invasion, which could be rescued by reexpression of an active, but not inactive PIP5KIγ90. Furthermore, PIP5KIγ90-deficient cells showed normal basal PI-4,5-P_2 levels in the plasma membrane but reduced the accumulation of PI-4,5-P_2 and talin at sites of *S. aureus* attachment and overall lower levels of FAK phosphorylation. These results highlight the importance of local synthesis of PI-4,5-P_2 by a focal adhesion-associated lipid kinase for integrin-mediated internalization of *S. aureus*.

KEYWORDS

fibronectin-binding protein, internalization, phosphatidylinositol-4,5-bisphosphate, phosphatidylinositol-4-phosphate-5-kinase, *Staphylococcus aureus*

1 | INTRODUCTION

Due to the rise in multidrug resistance, *Staphylococcus aureus*, a Gram-positive coccoid bacterium, is becoming a major healthcare challenge on a global scale (Liu et al., 2011; Sieradzki et al., 1999; Tsiodras et al., 2001; Turner et al., 2019). This microbial pathogen is able to cause a spectrum of diseases, from chronic manifestations such as abscesses, chronic osteomyelitis, or mastitis to life-threatening acute diseases such as endocarditis, sepsis, or toxic shock syndrome. *S. aureus* produces numerous bacterial surface-associated and secreted virulence factors, which allow the pathogen to adhere to and invade otherwise nonphagocytic cells, to evade immune detection, or to intoxicate host tissues (Arciola et al., 2018; Foster et al., 2014). Among staphylococcal adhesins, the cell wall-anchored fibronectin-binding proteins (FnBPs) play a particularly prominent role in host cell invasion (Foster, 2016; Hauck et al., 2012; Sinha et al., 1999). FnBPs can capture the glycoprotein fibronectin (Fn), which is an abundant constituent of human blood plasma

(Vuento & Vaheri, 1979). Soluble Fn adopts a closed, inactive conformation, where binding sites for receptors of the integrin family are inaccessible due to long-range intramolecular interactions between amino-terminal type I modules (FnI_{1-5}) and carboxy-terminal type III modules ($FnIII_{1-3}$ and $FnIII_{12-14}$) within the Fn homodimer (Henderson et al., 2011; Hymes & Klaenhammer, 2016; Vakonakis et al., 2009). Upon association of staphylococcal FnBP with Fn type I modules, intramolecular constraints are released exposing the integrin-binding motifs located in $FnIII_9$ and $FnIII_{10}$ (Marjenberg et al., 2010). As a consequence, FnBP-bound fibronectin is able to bind with high affinity to host receptors of the integrin family, such as integrin $\alpha_5\beta_1$, thereby tightly linking the bacteria with the host cell surface (Agerer et al., 2003; Sinha et al., 1999). FnBP-mediated Fn coating of the microorganisms clusters integrins, which in turn trigger canonical signaling events involving focal adhesion kinase (FAK) and Src family protein tyrosine kinases (PTKs) (Agerer et al., 2003, 2005; Fowler et al., 2003) and initiate the uptake of the bacteria by nonprofessional phagocytes such as fibroblasts, epithelial cells, and endothelial cells (Agerer et al., 2005; Brouillette et al., 2003; Dziewanowska et al., 1999; Konkel et al., 2020; Schroder et al., 2006).

Under physiological conditions, Fn-bound integrins initiate stable, localized multimeric protein complexes, so-called focal adhesions, which indirectly connect the intracellular domains of integrin heterodimers with the actomyosin cytoskeleton (Huveneers et al., 2008; Strohmeyer et al., 2017). Some of the structural integrin- or actin-associated proteins as well as F-actin are also recruited to Fn-coated *S. aureus* and are involved in the internalization of the bacteria (Agerer et al., 2005; Schroder et al., 2006). However, the regulatory checkpoints, which allow the bacteria to convert integrin-associated protein complexes into an endocytotic machinery, are currently unknown.

Interestingly, several of the integrin-associated proteins are regulated by phosphoinositides. In particular, phosphatidylinsositol (PtdIns)-4,5-bisphosphate (PI-4,5-P_2) does not only accumulate and help orchestrate the plasma membrane association of integrin-linked structural and signaling proteins such as talin, α-actinin, vinculin, or FAK (Chinthalapudi et al., 2018; Goni et al., 2014; Janmey, 1994; Martin, 1998) but also plays key roles in endocytosis and membrane trafficking (Daste et al., 2017; Mandal, 2020; Oppelt et al., 2013; Posor et al., 2015). In mammalian cells, PI-4,5-P_2 is mainly generated at the inner leaflet of the plasma membrane by the activity of type I PI-4-P 5-kinases (PIP5KIs) (van den Bout & Divecha, 2009). The three known members of the PIP5K family, PIP5KIα, PIP5KIβ, and PIP5KIγ (Jenkins et al., 1994; Kwiatkowska, 2010), preferentially phosphorylate the 5-hydroxyl position of PI-4-P to generate PI-4,5-P_2. PIP5KIα is enriched at the plasma membrane and the Golgi complex and has also been observed at sites of membrane ruffling induced by Rho GTPases. PIP5KIβ localizes to the plasma membrane and to vesicles in the perinuclear region of the cell (Di Paolo & De Camilli, 2006; Doughman et al., 2003). PIP5KIγ is present at the plasma membrane, with at least one isoform, the so-called PIP5KIγ90 or PIP5KIγ isoform #2, found to be enriched at focal adhesions and adherens junctions (Durand et al., 2016; Ling et al., 2002; Nader et al., 2016).

Take aways

- Fibronectin-binding *Staphylococcus aureus* induce accumulation of phosphoinositides at sites of host cell contact.
- Accumulation of phosphatidylinositol-4,5-bisphosphate (PI-4,5-P_2) is linked to *S. aureus* internalization.
- The integrin-associated enzyme PIP5KIγ90 is instrumental for local PI-4,5-P_2 production.
- Lack of PIP5KIγ90 impairs *S. aureus*-mediated integrin signaling and bacterial uptake.

With regard to bacterial internalization, PI-4,5-P_2 has been reported to either promote or inhibit the uptake of several bacteria. For example, PIP5KIα and PI-4,5-P_2 synthesis are instrumental for the cellular entry of *Chlamydia caviae* into HeLa cells (Dautry-Varsat et al., 2005). A positive role of PIP5KIα has also been reported for the internalization of *Yersinia pseudotuberculosis* (Wong & Isberg, 2003). In contrast, the Gram-negative pathogen *Shigella flexneri* injects the phosphoinositide phosphatase IpgD into the host cell, which dephosphorylates PI-4,5-P_2 and facilitates bacterial uptake (Niebuhr et al., 2002). Similarly, entry of *Salmonella typhimurium* and *Y. pseudotuberculosis* into host cells requires dephosphorylation of PI-4,5-P_2 to promote plasma membrane scission of the forming bacteria-containing vacuoles indicating that PI-4,5-P_2 hinders efficient internalization in these instances (Sarantis et al., 2012; Terebiznik et al., 2002).

In the case of *S. aureus*, however, it is unknown whether PI-4,5-P_2 is generated and whether it positively or negatively contributes to the integrin-mediated uptake of bacteria. We investigated this question in the present study and report that high levels of PI-4,5-P_2 occur at sites, where *S. aureus* engages with integrins. *S. aureus* internalization is reduced upon overexpression of a membrane-targeted PI-4,5-P_2-directed phosphatase or upon reduction of PIP5K activity. Moreover, deletion of the gene encoding the 90 kDa isoform of PIP5KIγ, which accumulates at integrin-rich sites associated with *S. aureus*, reduces both local PI-4,5-P_2 accumulation as well as bacterial internalization. Our results identify PI-4,5-P_2 as a positive contributor to host cell invasion by *S. aureus* and suggest that the lipid kinase PIP5KIγ serves as a regulator of integrin internalization.

2 | RESULTS

2.1 | PI-4,5-P_2 and PI-3,4,5-P_3 are enriched at the attachment sites of *S. aureus*

Previous studies have revealed that *S. aureus* triggers the recruitment and activation of integrin-associated signaling molecules (Hauck et al., 2012). To investigate, if staphylococcal engagement

of integrins is accompanied by elevated levels of phosphoinositides, we transfected 293 cells with vectors encoding GFP-tagged PH domains or with a GFP-only encoding vector (Balla, 2005; Balla & Varnai, 2009). The selected PH domains recognizing distinct phosphoinositides were expressed at comparable levels (Figure S1a,b, Supplementary Material). Cells were infected with the *S. aureus* strain Cowan, which exploits the FnBP-generated Fn coat to engage host integrin $\alpha_5\beta_1$. Upon *S. aureus* binding, GFP distribution in the cytosol remained unaltered (Figure 1). In contrast, the PH domains of Akt and Btk, which recognize phosphatidylinositol-3,4,5 trisphosphate (PI-3,4,5-P_3) and which were found at low levels at the cell periphery of uninfected cells, were strongly recruited to cell-associated *S. aureus* 2 hr after infection (Figure 1). Furthermore, the PH domain of PLCδ, which specifically binds phosphatidylinositol-4,5 bisphosphate (PI-4,5-P_2), became highly enriched around cell-associated bacteria (Figure 1). In contrast, the phosphatidylinositol-4 phosphate (PI-4-P) and Arf-1-binding PH domain of OSBP, which directs this protein to the trans-Golgi-network (Levine & Munro, 2002), was not altered in its distribution upon *S. aureus* infection (Figure 1). These results indicated that PI-4,5-P_2 and PI-3,4,5-P_3 accumulate at *S. aureus*–host cell attachment sites. As PI-4,5-P_2 is involved in regulating integrin-associated focal adhesion proteins, we concentrated on this phosphoinositide.

2.2 | PI-4,5-P_2 enrichment at the attachment sites of *S. aureus* is not a consequence of increased membrane volume

To confirm that the observed enrichment of PI-4,5-P_2 is not due to an increased overall volume of plasma membrane around cell-associated bacteria, we coexpressed a membrane-anchored red fluorescent protein (mKate-CAAX) together with either PLCδ-PH-GFP or GFP and infected the cells for 2 hr with pacific-blue stained *S. aureus* (Figure 2a). While the PLCδ-PH-GFP signal was enriched around *S. aureus*, mKate-CAAX showed a patchy distribution in the plasma membrane but was not enriched around cell-associated bacteria (Figure 2a). To better delineate the bulk plasma membrane, cells expressing GFP or PLCδ-PH-GFP were additionally stained with the membrane dye Cellmask Orange, which uniformly labeled the

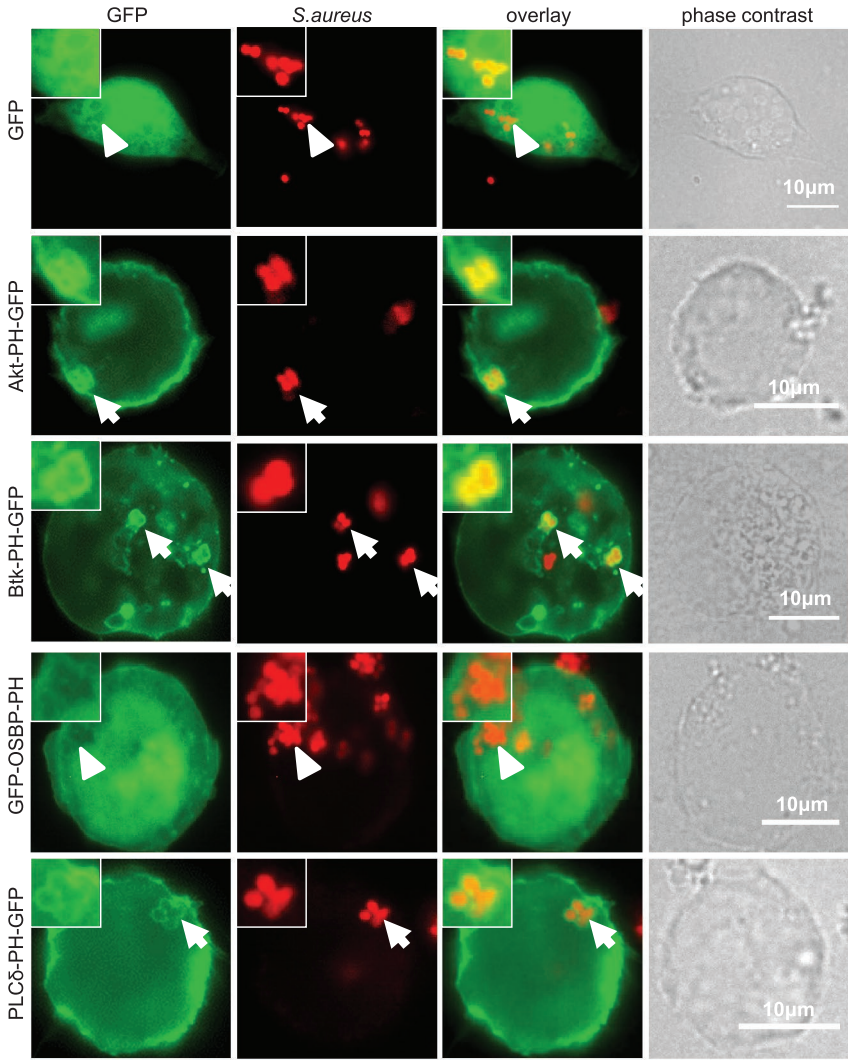

FIGURE 1 PI-4,5-P_2 and PI-3,4,5-P_3 are recruited to the attachment sites of *Staphylococcus aureus*. 293 cells were transfected with constructs encoding GFP or the indicated PH domains fused to GFP. Twenty-four hours after transfection, cells were seeded on poly-L-lysine-coated coverslips and infected with rhodamine-labeled *S. aureus* for 2 hr before fixation. The unaltered distribution of GFP, as well as OSBP-PH-GFP (arrowheads) and recruitment of various PH-domain-GFP-fusion proteins to cell-associated bacteria (arrows), was visualized by widefield fluorescence microscopy. Bar, 10 µm

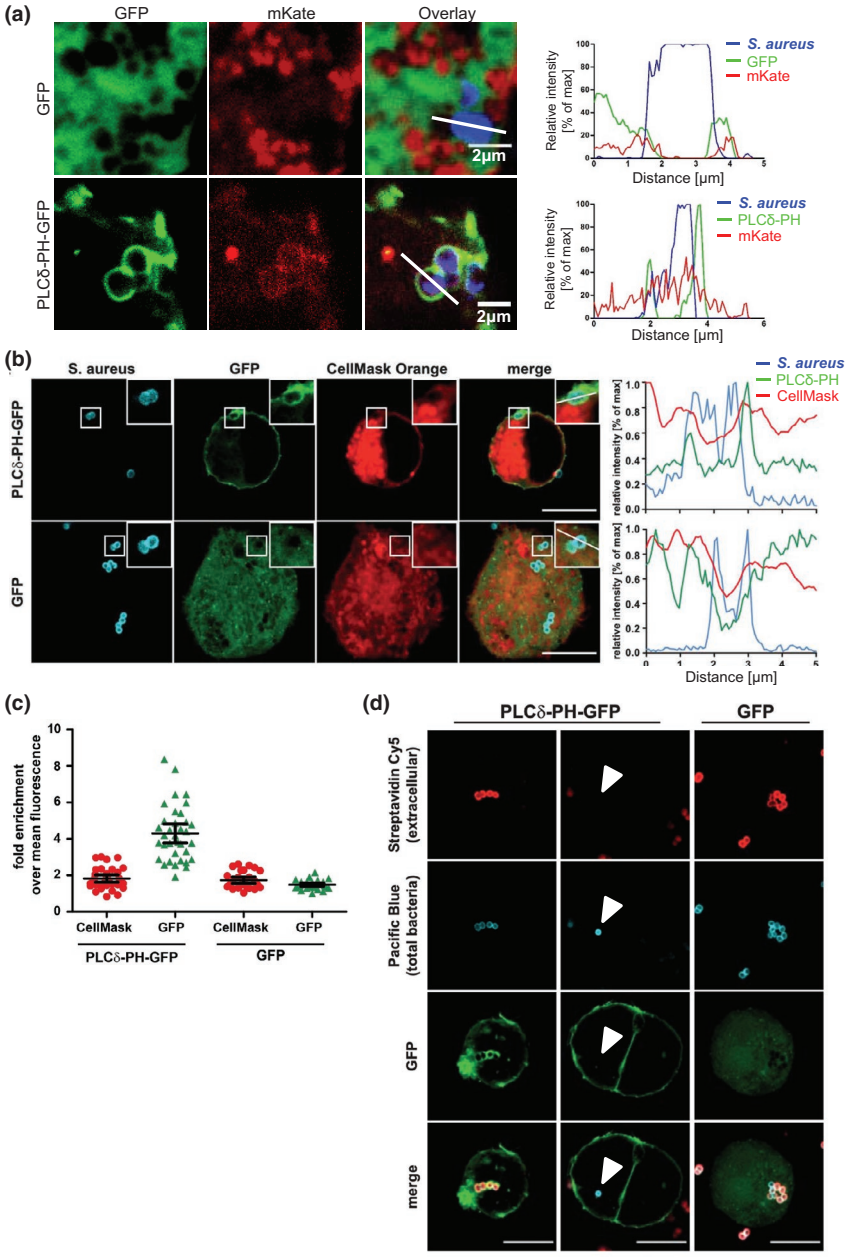

FIGURE 2 PI-4,5-P_2 accumulates around cell-associated *Staphylococcus aureus*. (a) 293 cells were cotransfected with pcDNA3.1-mKate-CAAX together with GFP or PLCδ-PH-GFP. Twenty-four hours after transfection, cells were seeded on poly-lysine-coated coverslips and infected with pacific blue-labeled *S. aureus* for 2 hr. Using confocal microscopy, the recruitment of mKate-CAAX, GFP, or PLCδ-PH-GFP to cell-attached bacteria (blue) was monitored. Fluorescence intensity profiles (right graphs) along with the line indicated in the overlay picture show the strong enrichment of PLCδ-PH-GFP versus mKate-CAAX around *S. aureus* (blue). (b) 293 cells were transfected with PLCδ-PH-GFP or GFP, infected with pacific blue-labeled *S. aureus*, and stained with a membrane dye (CellMask Orange). Fluorescence intensity profiles along with the line show that the PLCδ–PH-GFP recruitment is not due to membrane volume effects. Scale bars, 10 μm. (c) Quantification of the experiment in (b). 25–35 individual infection sites were analyzed by measuring the maximum intensity of the CellMask Orange stain or GFP at the site and dividing it by the mean fluorescence intensity of the whole cell. The fold enrichment over the mean fluorescence of the respective fluorophores is given. Error bars indicate 95% confidence intervals. (d) *S. aureus* were labeled with pacific blue and Sulfo-NHS-Biotin and used for infection of PLCδ-PH-GFP or GFP transfected 293 cells. Following infection, extracellular bacteria were additionally labeled with Streptavidin-Cy5. Shown are representative PLCδ-PH-GFP expressing cells with cell-associated *S. aureus* (left row) or internalized *S. aureus* (middle row; arrowhead). No recruitment of GFP was seen (right row). Scale bars, 10 μm

plasma membrane (Figure 2b). Again, PLCδ-PH-GFP, but not GFP, showed a clear enrichment around *S. aureus*–host cell contact sites (Figure 2b). Quantification of the relative fluorescence intensities at these contact sites versus other areas of the cell membrane revealed that PH-PLCδ-GFP was ~5-fold enriched around the pathogens, whereas the general membrane stain showed only a minor

increase (~1.9-fold) in fluorescence around cell-associated bacteria (Figure 2c). These data indicate that the membrane volume around cell-attached bacteria slightly increases, as expected for an endocytic process, but that there is a much more prominent elevation in PI-4,5-P_2 levels at these sites (Figure 2c). Moreover, the accumulation of PI-4,5-P_2 around the bacteria occurred upon contact with the host cell, when the microbes were still extracellular, whereas the PLCδ-PH-GFP signal around the bacteria was lost upon internalization (Figure 2d). Together, these data demonstrate that PI-4,5-P_2 accumulates at *S. aureus*–host cell attachment sites.

2.3 | PI-4,5-P_2 accumulation is induced by FnBP-mediated integrin engagement

In contrast to nonpathogenic members of the genus *Staphylococcus*, *S. aureus* can recruit Fn and thereby engage integrins on the cell surface. To test whether the observed accumulation of the PI-4,5-P_2-binding PLCδ-PH-GFP is due to integrin engagement, cells were infected with *S. aureus* or the nonpathogenic, non-Fn-binding *S. carnosus*, respectively. Whereas infection with *S. aureus* resulted in a strong accumulation of PLCδ-PH-GFP, the rare contact sites

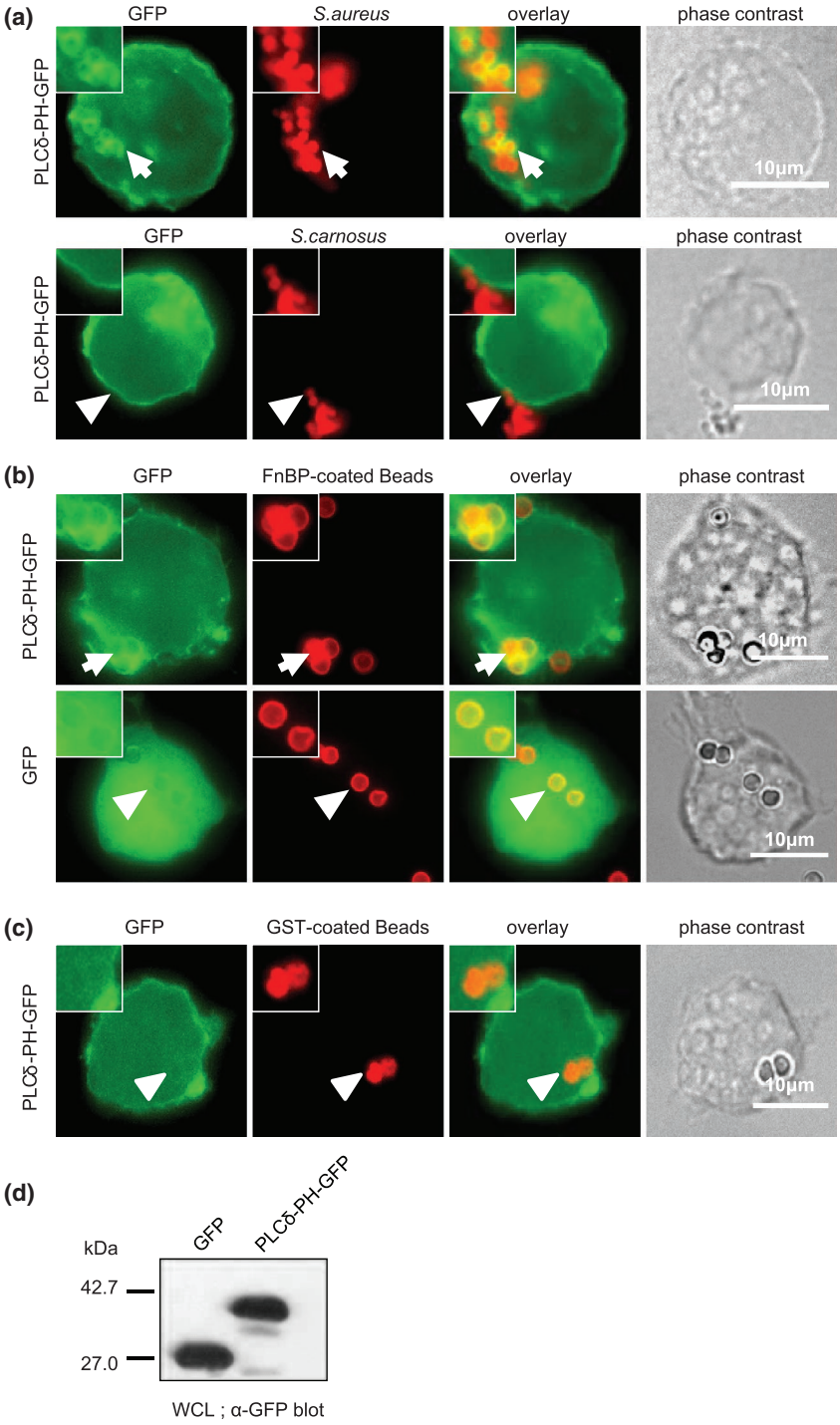

FIGURE 3 PI-4,5-P_2 accumulation is induced by FnBP-mediated integrin engagement. (a) 293 cells were transfected with PLCδ-PH-GFP, then infected by rhodamine stained *Staphylococcus aureus* or *S. carnosus* for 2 hr, respectively. Infected samples were fixed and observed by widefield microscopy. Recruitment of PLCδ-PH-GFP is seen around cell-associated *S. aureus* (arrows) but not *S. carnosus* (arrowheads). (b, c) 293 cells were transfected with vectors encoding PLCδ-PH-GFP or GFP, respectively. Transfected cells were incubated with FnBP-coated (b) or GST-coated (c) microbeads for 2 hr. After incubation, cells were fixed and analyzed as in (a). PLCδ-PH-GFP (arrows), but not GFP (arrowheads), was recruited to GST-FnBP-coated beads (b), whereas GST-coupled beads did not lead to recruitment of PLCδ-PH-GFP (c). Bar, 10 μm. (d) Expression of GFP and PLCδ-PH-GFP by transfected 293 cells was detected by Western Blotting with a monoclonal anti-GFP antibody

of *S. carnosus* with host cells did not show recruitment of PLCδ-PH-GFP (Figure 3a). To test whether bacterial binding via FnBP to integrins is sufficient to induce increased PI-4,5-P_2 levels around cell-associated bacteria, the fibronectin-binding domains of FnBP were expressed as GST-fusion protein in *Escherichia coli*, purified, covalently attached to microbeads and then added to 293 cells expressing the GFP-tagged PLCδ PH domain or GFP only. Similar to the intact, Fn-binding *S. aureus*, GST-FnBP-coated beads triggered PLCδ PH-GFP recruitment, whereas GFP distribution within the cell remained unaltered (Figure 3b). As expected, microbeads coated with GST associated poorly with cells and did not result in accumulation of PLCδ-PH-GFP (Figure 3c). Equivalent expression levels of PLCδ PH-GFP or GFP were verified by Western blotting (Figure 3d). Altogether, these findings demonstrate that FnBP-mediated host cell contact by *S. aureus* is sufficient to trigger a local elevation in PI-4,5-P_2 levels.

2.4 | Reduction of plasma membrane PI-4,5-P_2 inhibits *S. aureus* invasion

To investigate if the elevated PI-4,5-P_2 levels observed in the vicinity of cell-associated *S. aureus* are relevant for the internalization of the bacteria, we attempted to directly interfere with the plasma membrane pools of PI-4,5-P_2 by overexpressing a PI-4,5-P_2 consuming enzyme. To this end, we fused the myristoylation sequence derived from the Src family kinase Lyn and GFP to the intact phosphatase domain of the 5′-inositol phosphatase INPP5J (myrINPP5J-GFP) or to a phosphatase-inactive INPP5J (myrINPP5J-ia-GFP). The resulting proteins were expressed at equivalent levels by 293 cells (Figure S2a). The transfected cells were infected with *S. aureus* for 2 hr and differentially stained for intra- and extracellular bacteria (Figure S2b) to quantify the total cell-associated and the internalized bacteria. While the total number of cell-associated bacteria was similar in the different samples, expression of active myrINPP5J slightly, but consistently reduced the internalization of *S. aureus* (Figure 4a,b). To investigate if the active myrINPP5J affects PI-4,5-P_2 levels at the bacterial attachment sites, cells were cotransfected with either myrINPP5J or myrINPP5J-ia fused to the blue fluorescent protein Cerulean together with PLCδ PH-GFP. PI-4,5-P_2 accumulation around *S. aureus* was less pronounced in myrINPP5J expressing cells compared with cells expressing myrINPP5J-ia or the isolated Cerulean, while the total cellular levels of PI-4,5-P_2 were only marginally reduced (Figure 4c). The overexpression of myrINPPJ5 lowered PLCδ PH-GFP accumulation by about 40% (Figure 4d). This partial effect might be due to the predominant localization of myrINPP5J to internal membranes (Figure S2b), rather than to the plasma membrane, where *S. aureus* internalization is taking place. Nevertheless, the results with myrINPP5J overexpression indicated that the increased levels of PI-4,5-P_2 found around cell-associated *S. aureus* contribute to bacterial internalization.

2.5 | PIP5KIγ promotes the uptake of *S. aureus*

PI-4,5-P_2 can be generated by the action of PIP kinases or by dephosphorylation of PI-3,4,5-P_3. The major contributors to the generation of plasma membrane PI-4,5-P_2 pools comprise the enzymes of the type I phosphatidylinositol 4-phosphate 5-kinase (PIP5KI) family (Mayinger, 2012). In humans, the PIP5KI family consists of three isozymes, α, β, and γ (Ishihara et al., 1996, 1998; Loijens & Anderson, 1996). To investigate, which of these three enzymes contributes to *S. aureus* host cell invasion, we efficiently depleted the different PIP5KIs mRNAs in HeLa cells using specific siRNAs (Figure 5a), infected the resulting cells with *S. aureus* or *S. carnosus*, and determined the number of total cell-associated as well as of viable intracellular bacteria (Figure 5b). Interestingly, the amount of total cell-associated bacteria between control cells and the different knock-down cells was comparable (Figure 5b), suggesting that the surface expression and ligand binding ability of integrin $\alpha_5\beta_1$ was not affected by the depletion of either enzyme. While the number of viable intracellular bacteria was unaltered in PIP5KIβ-knockdown cells, the recovered intracellular bacteria were significantly decreased in PIP5KIγ- and PIP5KIα-knockdown cells (Figure 5b). As PIP5KIγ is known to interact with proteins at integrin-based focal adhesion sites, we focused our attention on this enzyme. First, we investigated the subcellular location of PIP5KIγ during bacterial uptake by expressing a GFP-tagged wild type or a kinase-inactive form of PIP5KIγ in 293 cells (Figure S3). Both the wild type and the inactive form of PIP5KIγ localized to the plasma membrane, while, in particular, the wildtype enzyme showed a prominent, more than 10-fold enrichment around the *S. aureus* attachment sites (Figure 5c,e). Clearly, an accumulation of PIP5KIγ was not observed upon infection with *S. carnosus* (Figure 5d). Collectively, these data indicate that PIP5KIγ localizes to sites of *S. aureus* internalization and support the idea that this enzyme provides local PI-4,5-P_2 production.

2.6 | Deletion of the PIP5KIγ talin-binding site impairs uptake of *S. aureus*

In mammalian cells, there are two main isoforms of PIP5KIγ, which are named, according to their molecular size, PIP5KIγ90 or PIP5KIγ87 (Figure 6a). Due to alternative splicing, the PIP5KIγ87-encoding transcript skips exon 17 and therefore lacks a 26 amino acid motif near the carboxy-terminus (van den Bout & Divecha, 2009). This short amino acid stretch binds to the integrin-associated protein talin and is important to localize PIP5KIγ90 to integrin-rich focal adhesion sites (Di Paolo et al., 2002). There, PIP5KIγ90 is involved in a local production of PI-4,5-P_2 (Ling et al., 2002). Interestingly, mice with a genetic deletion of exon 17 of the *pip5klγ* gene (PIP5KIγ90$^{-/-}$) are viable and fertile and express PIP5KIγ87 but lack the PIP5KIγ90 isoform (Legate et al., 2012). To directly test the role of PIP5KIγ90 and its 26aa talin-binding motif, we established murine embryonic fibroblasts (MEFs) derived from mice carrying a floxed exon 17 of the *pip5klγ* gene (PIP5KIγ90$^{fl/fl}$ control cells) or lacking exon 17

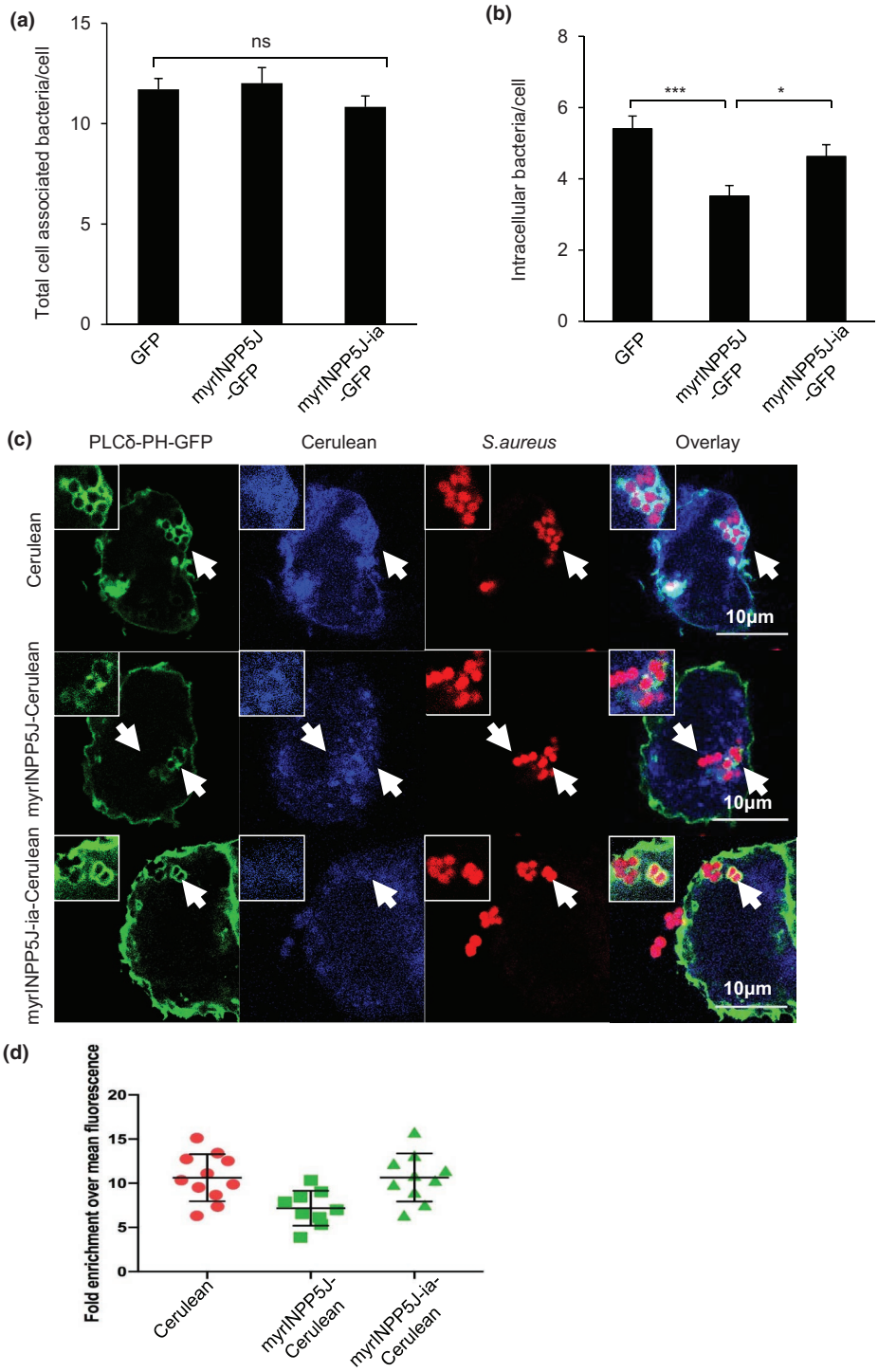

FIGURE 4 Expression of a membrane-targeted 5′-PIP phosphatase domain decreases *Staphylococcus aureus* internalization. (a and b) 293 cells were transfected with GFP, the membrane-targeted phosphatase domain of INPP5J (myrINPP5J-GFP), or the inactive phosphatase (myrINPP5J-ia-GFP), respectively. Twenty-four hours after transfection, 2×10^5 cells were seeded on poly-L-lysine-coated coverslips and infected the next day with pacific blue-stained and biotin-labeled *S. aureus* for 2 hr. After fixation, samples were incubated with streptavidin-AlexaFluor647 to mark extracellular bacteria. Total cell-associated (a) or intracellular (b) bacteria were quantified in three independent samples ($n = 3$ samples; at least 70 cells/sample). Bars represent mean ± *SEM* of bacteria/cell; unpaired *t* test. $^{***}p < .001$, $^{*}p < .05$. (c) 293 cells were cotransfected with PLCδ-PH-GFP together with Cerulean, the membrane-targeted phosphatase domain of INPP5J (myrINPP5J-Cerulean), or the inactive phosphatase (myrINPP5J-ia-Cerulean), respectively. Twenty-four hours after transfection, 2×10^5 cells were seeded on poly-L-lysine-coated coverslips and the next day infected with rhodamine-stained *S. aureus* for 2 hr. Fixed samples were analyzed by confocal microscopy, arrows point to *S. aureus*-cell attachment sites, which show reduced recruitment of PLCδ-PH-GFP in cells expressing myrINPP5J-Cerulean. (d) PLCδ-PH-GFP enrichment at infection sites of cells from (c) was analyzed by measuring the maximum GFP intensity at the infection site and dividing it by the mean fluorescence intensity of the whole cell. The fold enrichment of 9–11 individual sites is shown in the scatter plot with bars indicating the mean fold enrichment and error bars indicate 95% confidence intervals

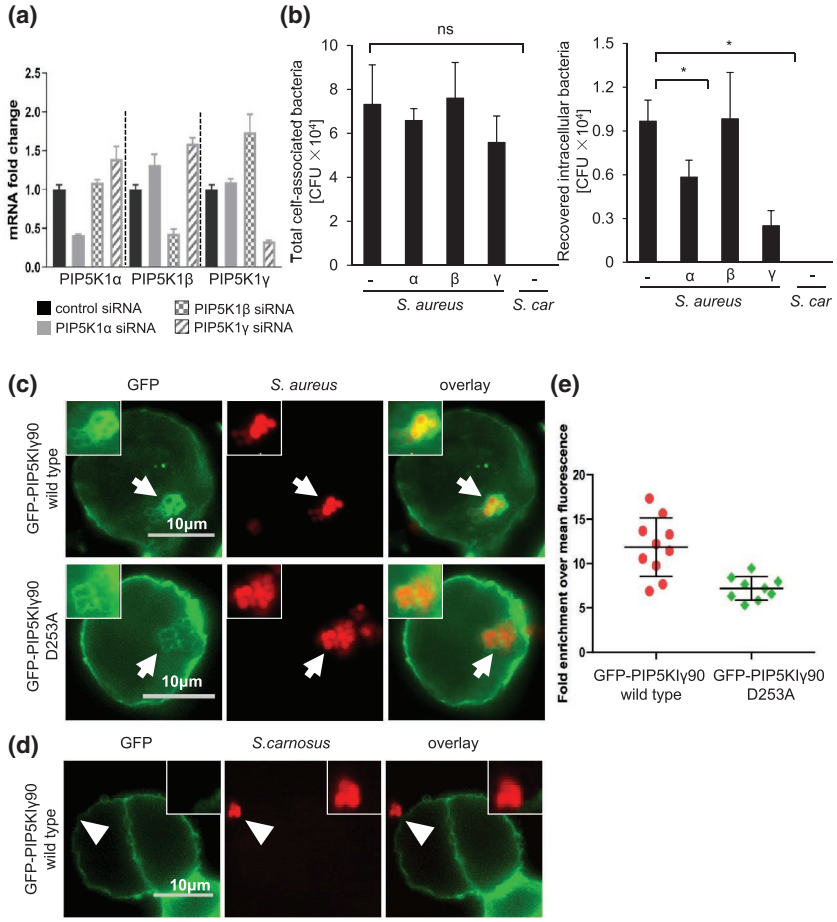

FIGURE 5 PIP5KIγ is involved in the integrin-mediated uptake of *Staphylococcus aureus*. (a) HeLa cells were transfected with siRNA against PIP5KIα, β, γ, or with control siRNA, respectively. Forty-eight hours later, total RNA was isolated and the mRNA level for each PIP5KI transcript was analyzed by qRT-PCR. PIP5KI transcription was normalized to GAPDH level and the *Ct* values from control knockdown samples are used to calculate the fold change of mRNA levels. Bars represent the mean ± *SEM* of three independent experiments each performed in triplicate. (b) siRNA-transfected HeLa cells were infected for 2 hr with *S. aureus* or *S. carnosus*, respectively. Total cell-associated or intracellular bacteria were quantified by gentamicin protection assay. The bars show mean values ± *SEM* of three independent experiments. Samples were compared with control knockdown cells infected with *S. aureus* and significance was evaluated by an unpaired *t* test. $^*p < .05$. (c, d) 293 cells were transfected as indicated with the GFP-tagged active (PIP5KIγ90 wild type) or the enzymatic inactive form of PIP5KIγ (PIP5KIγ90 D253A). Transfected cells were infected with rhodamine-labeled *S. aureus* (c) or *S. carnosus* (d), respectively. Two hours later, the samples were fixed and analyzed by confocal microscopy. The recruitment of GFP-PIP5KIγ90 wild type and GFP-PIP5KIγ90 D253A in response to *S. aureus* infection is indicated by arrows (c), whereas *S. carnosus* does not lead to altered distribution of GFP-PIP5KIγ90 (d; arrowhead). (e) Local accumulation of GFP-PIP5KIγ90 wild type and GFP-PIP5KIγ90 D253A at infection sites of cells from (c) was analyzed by measuring the maximum GFP intensity at the infection site and dividing it by the mean fluorescence intensity of the whole cell. The fold enrichment of 9–10 individual sites is shown in the scatter plot with bars indicating the mean fold enrichment and error bars indicate 95% confidence intervals

(PIP5KIγ90$^{-/-}$). We confirmed the deletion of exon 17 by genotyping (Figure 6b) and verified similar expression levels of fibronectin-binding integrins $\alpha_5\beta_1$ and $\alpha_V\beta_3$ as well as integrin-associated proteins by flow cytometry or Western blotting, respectively (Figure S4a,b). PIP5KIγ90$^{fl/fl}$ control and PIP5KIγ90$^{-/-}$ cells were infected with *S. aureus* for 2 hr, fixed, and differentially stained for intra- and extracellular bacteria (Figure 6c,d). Quantification of total cell-associated or intracellular bacteria in PIP5KIγ90$^{fl/fl}$ versus PIP5KIγ90$^{-/-}$ cells demonstrated that bacterial binding occurred at a similar level, but the number of intracellular bacteria in PIP5KIγ90$^{-/-}$ cells was significantly lower than in PIP5KIγ90$^{fl/fl}$ cells (Figure 6d). Similar results were obtained by gentamicin protection assays. Again, the levels of total cell-associated bacteria did not differ, while less viable intracellular bacteria were recovered from PIP5KIγ90$^{-/-}$ cells compared with PIP5KIγ90$^{fl/fl}$ cells (Figure 6e). Together, these results demonstrate that PIP5KIγ90 is responsible for local production of PI-4,5-P_2 to allow optimal integrin-mediated uptake of *S. aureus*.

2.7 | Reexpression of PIP5KIγ90 in PIP5KIγ90$^{-/-}$ fibroblasts rescues uptake of bacteria

To confirm the contribution of PIP5KIγ90 to integrin-mediated internalization of *S. aureus*, the PIP5KIγ90$^{-/-}$ cells were complemented by transiently expressing comparable levels of GFP-tagged PIP5KIγ90, the inactive version of PIP5KIγ90 (PIP5KIγ90 D253A) or GFP-only

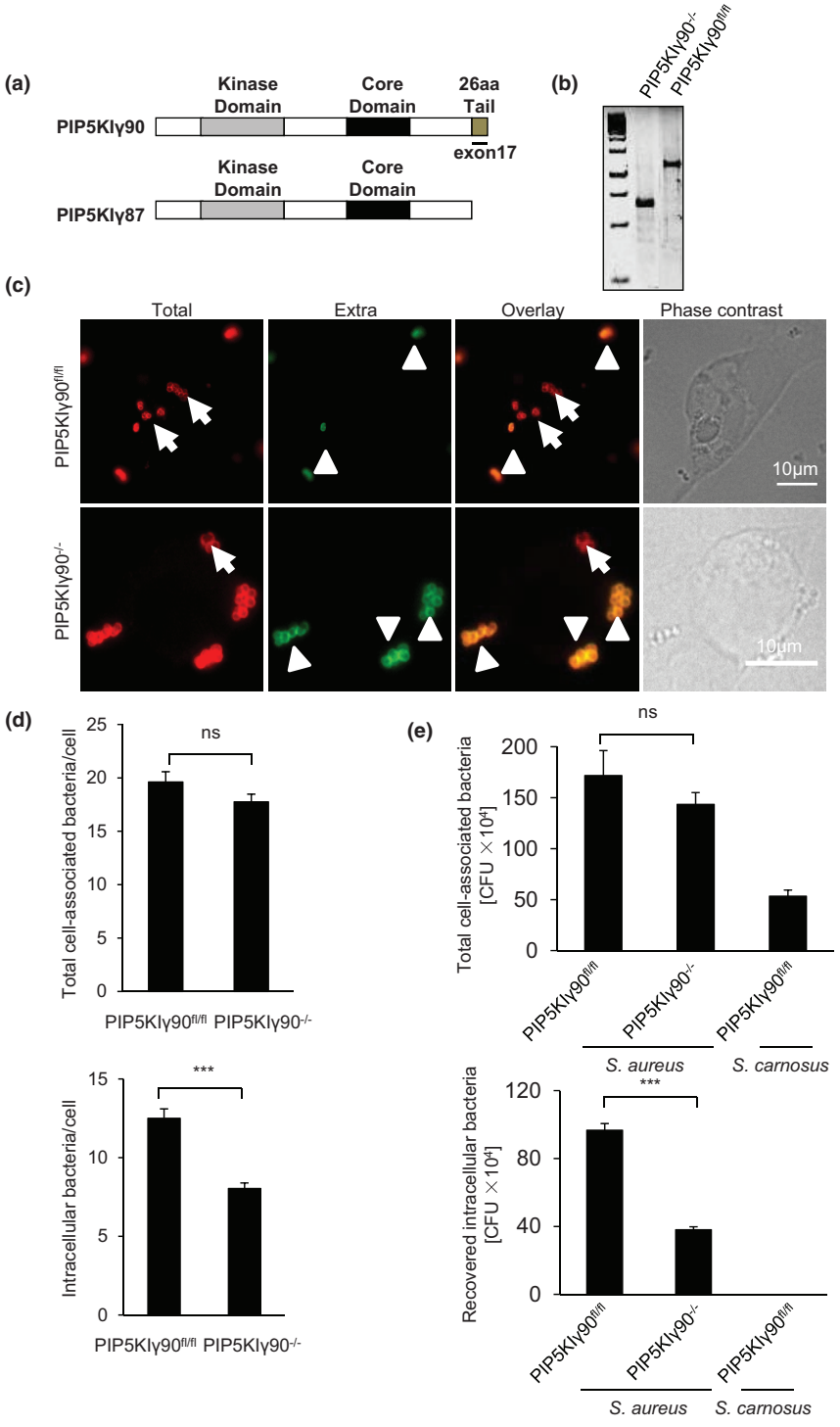

FIGURE 6 Deletion of the PIP5K talin-binding site in fibroblasts impairs uptake of *Staphylococcus aureus*. (a) Schematic view of the two major PIP5KIγ isoforms, PIP5KIγ90 and PIP5KIγ87, and the location of exon 17. (b) Genomic DNA of PIP5KIγ90$^{-/-}$ and PIP5KIγ90$^{fl/fl}$ cells was analyzed by PCR for the absence of exon 17. (c) PIP5KIγ90$^{-/-}$ and PIP5KIγ90$^{fl/fl}$ cells were infected with *S. aureus* for 2 hr. Fixed samples were differentially stained to distinguish the extracellular (red and green staining, arrowheads) and intracellular bacteria (red staining only; arrows). Bars, 10 μm. (d) Experiments were performed as in (c) and the number of total cell-associated (upper panel) or intracellular bacteria (lower panel) per cell was quantified (at least 100 cells/sample). Significance was evaluated by an unpaired *t* test. ***$p < .001$. (e) PIP5KIγ90$^{fl/fl}$ and PIP5KIγ90$^{-/-}$ cells were infected with *S. aureus* or *S. carnosus*, respectively, for 2 hr. The total cell-associated and recovered intracellular bacteria were quantified by gentamicin protection assay. The bars show mean values ± *SEM* of three independent experiments. Significance was evaluated by an unpaired *t* test. ***$p < .001$

(Figure S4c). These cells were infected with *S. aureus*, fixed, and differentially stained for extra- and intracellular bacteria (Figure 7a). Enumeration of bacteria in these transfected cells by microscopy revealed that the number of cell-associated bacteria was similar in all the samples (Figure 7b). However, the internalization of *S. aureus* by PIP5KIγ90$^{-/-}$ cells was clearly diminished compared with wild-type cells (Figure 7b). Importantly, the uptake of *S. aureus* was rescued in PIP5KIγ90$^{-/-}$ cells reexpressing the wild-type PIP5KIγ90 enzyme, whereas reexpression of the kinase-inactive enzyme or expression of GFP-only did not increase the numbers of intracellular *S. aureus* (Figure 7a,b). These results corroborate the functional role of PIP5KIγ90 and its enzyme activity in the integrin-mediated uptake of *S. aureus*.

2.8 | The talin-binding site of PIP5KIγ promotes the enrichment of PI-4,5-P_2 and talin at bacterial attachment sites

Since PIP5KIγ was recruited to the cell-attached bacteria, we wondered whether this enzyme is responsible for the elevated PI-4,5-P_2

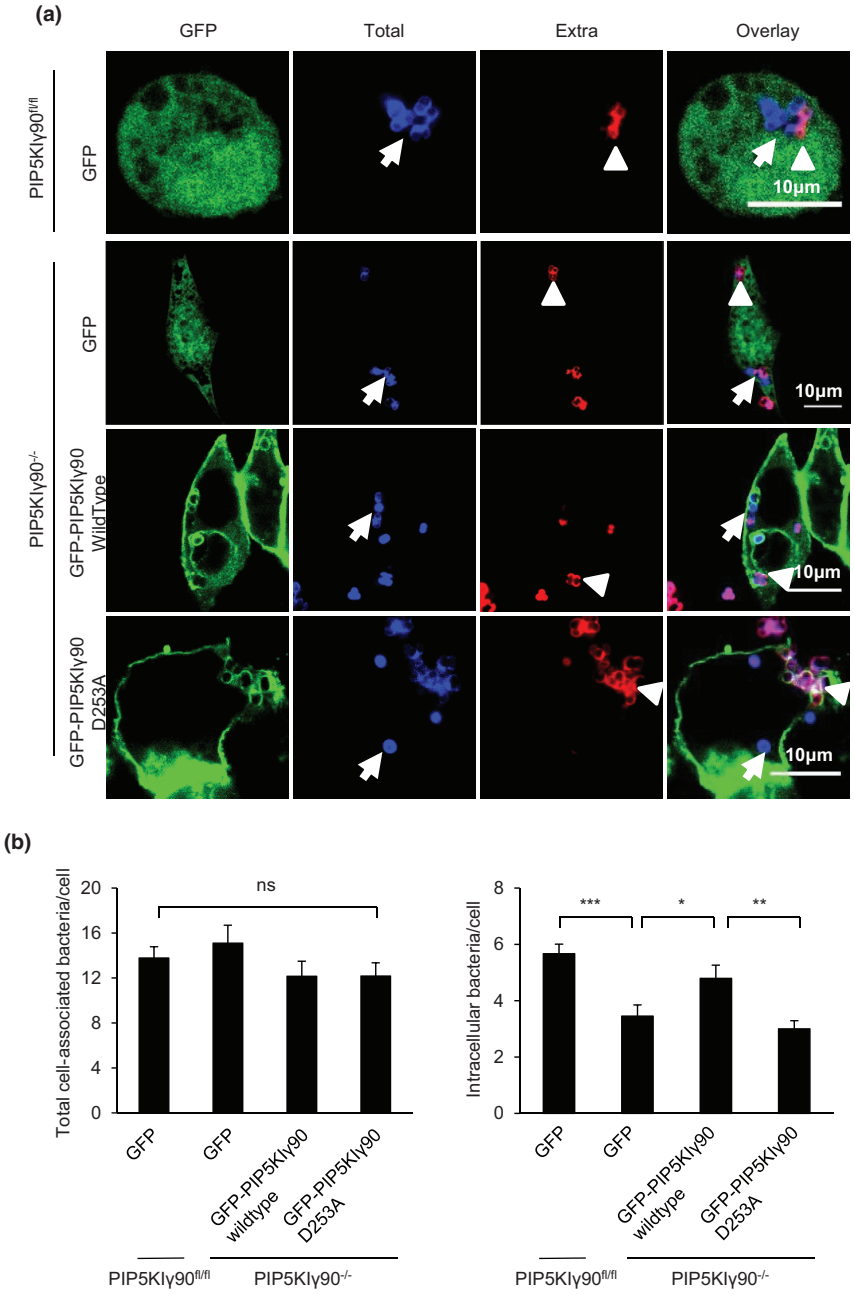

FIGURE 7 Reexpression of active PIP5KIγ90 in PIP5KIγ90$^{-/-}$ fibroblasts rescues bacterial uptake. (a) PIP5KIγ90$^{-/-}$ cells were transfected with plasmids encoding GFP, GFP-PIP5KIγ90 wild type, or a kinase-inactive mutant of PIP5KIγ90 (PIP5KIγ90 D253A), respectively. As a control, PIP5KIγ90$^{fl/fl}$ cells were transfected with GFP. Twenty-four hours after transfection, cells were infected with pacific blue-stained and biotin-labeled *Staphylococcus aureus* for 2 hr. After fixation, samples were stained with streptavidin-AlexaFluor647 to mark extracellular bacteria. Arrows indicate examples of intracellular bacteria stained in blue only, whereas arrowheads point to examples of extracellular bacteria stained in blue and red. (b) Experiments were performed as in (a) and the number of total cell-associated (left panel) or intracellular bacteria (right panel) per cell was quantified ($n = 3$ samples; at least 30 cells/sample). Bars show the mean values ± *SEM* from three independent experiments. Significance was evaluated by Student's *t* test. $^{***}p < .001$, $^{**}p < .01$, $^{*}p < .05$

FIGURE 8 PIP5KIγ90$^{-/-}$ fibroblasts lack local PI-4,5-P_2 production and talin accumulation upon *Staphylococcus aureus* infection. (a) PIP5KIγ90$^{fl/fl}$ and PIP5KIγ90$^{-/-}$ cells were transfected with GFP or PLCδ-PH-GFP, respectively. Forty-eight hours after transfection, cells were infected for 2 hr with rhodamine-labeled *S. aureus*. Upon fixation, recruitment of GFP or PLCδ-PH-GFP was monitored by confocal fluorescence microscopy. Recruitment of PLCδ-PH-GFP in PIP5KIγ90$^{fl/fl}$ cells is indicated by arrows, whereas the absence of GFP or PLCδ-PH-GFP recruitment to bacterial attachment sites is marked by arrowheads. (b) Quantification of GFP fluorescent intensity in samples from (a). The maximum GFP intensity at the infection site was divided by the mean fluorescence intensity of the whole cell. The fold enrichment of 6–8 individual sites is shown. Bars indicate mean fold enrichment and error bars indicate 95% confidence intervals. (c) PIP5KIγ90$^{fl/fl}$ cells were transfected with PLCδ-PH-GFP, infected with *S. carnosus*, and evaluated as in (a). The arrowhead indicates the lack of PLCδ-PH-GFP in the few *S. carnosus*–host cell attachment sites. (d) PIP5KIγ90$^{fl/fl}$ and PIP5KIγ90$^{-/-}$ cells were transfected with GFP or GFP-Talin, respectively. Cells were infected and analyzed by confocal microscopy for GFP or GFP-Talin recruitment as in (a). (e) Quantification of GFP or GFP-talin fluorescence intensity in samples from (d). The maximum intensity at the infection site was divided by the mean fluorescence intensity of the whole cell. The fold enrichment of 6–8 individual sites is shown. Bars indicate mean fold enrichment and error bars indicate 95% confidence intervals. (f) GFP intensity profiles at bacterial attachment sites (indicated by the white line in (d)) highlight the enrichment of GFP-talin in PIP5KIγ90$^{fl/fl}$ cells (middle graph) compared with the minor enrichment of GFP-talin in PIP5KIγ90$^{-/-}$ cells (lower graph) and the absent enrichment of GFP in PIP5KIγ90$^{fl/fl}$ cells (upper graph)

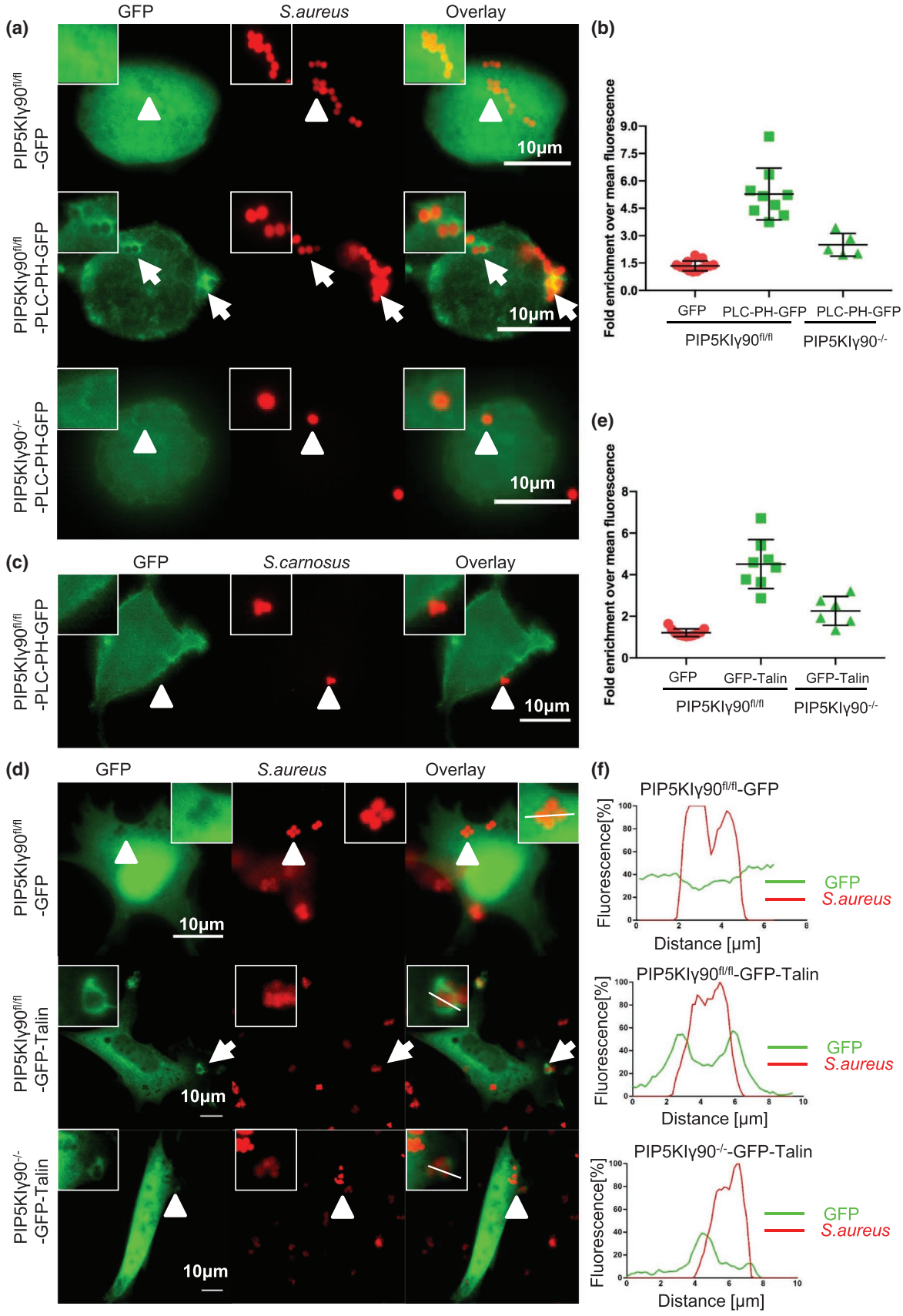

levels during bacterial internalization. Expression of the GFP-tagged PLCδ-PH domain suggests that the PI-4,5-P_2 levels are about 5-fold enriched around cell-bound *S. aureus* in PIP5KIγ90$^{fl/fl}$ cells (Figure 8a,b). Live-cell imaging demonstrated the transient nature of the increase in PI-4,5-P_2, which was most pronounced within 1–5 min upon *S. aureus* contact with the host cell (Figure S5). GFP

alone showed only marginal (1.5-fold) enrichment around *S. aureus* associated with PIP5KIγ90$^{fl/fl}$ cells (Figure 8a,b). In contrast to the situation in PIP5KIγ90$^{fl/fl}$ cells, PIP5KIγ90$^{-/-}$ cells showed strongly reduced (2-fold) accumulation of PLCδ-PH around *S. aureus* (Figure 8a,b). *S. carnosus*, which does not engage integrins, did not influence PLCδ-PH distribution (Figure 8c). As the talin FERM domain is a binding partner of the C-terminal 26 amino acid extension in PIP5KIγ90, we wondered whether talin accumulation is altered in PIP5KIγ90$^{-/-}$ cells. To address this question, PIP5KIγ90$^{fl/fl}$ and PIP5KIγ90$^{-/-}$ cells were transiently transfected with GFP-tagged talin and, as a negative control, PIP5KIγ90$^{fl/fl}$ cells with GFP-only, and their expression monitored by Western blotting (Figure S4d). Transfected cells were infected with rhodamine-labeled *S. aureus* for 2 hr. In PIP5KIγ90$^{fl/fl}$ cells, GFP-talin was recruited upon contact with *S. aureus* (Figure 8d–f). In contrast, GFP-talin accumulation around cell-associated bacteria was almost completely absent in PIP5KIγ90$^{-/-}$ cells (Figure 8d–f). Combined these results indicate that PIP5KIγ90 is responsible for local production of PI-4,5-P_2 at the bacterial attachment sites, which is important for talin recruitment to bacteria engaged integrins.

2.9 | PIP5KIγ90 is critical for maximal FAK activity in response to integrin stimulation

Several signaling processes, including activation of the protein tyrosine kinase FAK as well as phosphorylation of FAK-binding partners, such as paxillin or cortactin, occur upon integrin engagement by *S. aureus* (Agerer et al., 2005). To monitor such downstream signaling events, PIP5KIγ90$^{fl/fl}$ or PIP5KIγ90$^{-/-}$ cells were either infected with *S. aureus* for different time periods or left uninfected. Western blot analysis of whole-cell lysates with phospho-tyrosine-specific antibodies revealed that overall tyrosine phosphorylation was reduced in uninfected PIP5KIγ90$^{-/-}$ compared with the PIP5KIγ90 expressing cells (Figure 9a). Moreover, PIP5KIγ90 expressing cells showed a clear increase in tyrosine phosphorylation, and in particular in tyrosine phosphorylation of FAK at the autophosphorylation site Y397, during 2 hr upon *S. aureus* infection (Figure 9a,b). The increase in FAK tyrosine phosphorylation was strongly diminished, and phosphorylation of Y397 was almost completely absent in cells lacking PIP5KIγ90 (PIP5KIγ90$^{-/-}$ cells) (Figure 9a,b). These results indicate that maximal activation of tyrosine phosphorylation of FAK downstream of integrin engagement by *S. aureus* requires PIP5KIγ90 activity. Further reducing FAK activity by pharmacological inhibition with the FAK-specific inhibitor PF431396 led to a complete abrogation of *S. aureus* invasion into wild-type and PIP5KIγ90$^{-/-}$ MEFs (Figure 9c), suggesting that local PI-4,5-P_2 production by PIP5KIγ90 is one of several stimulatory inputs for maximal FAK activity. To investigate, if maximal FAK Y397 phosphorylation requires PIP5KIγ90 activity during physiological stimulation of integrins upon cell-matrix adhesion, PIP5KIγ90$^{fl/fl}$ or PIP5KIγ90$^{-/-}$ cells were plated on fibronectin-coated dishes or were kept in suspension. Clearly, cell adhesion to fibronectin stimulated a strong increase in tyrosine phosphorylation in both PIP5KIγ90$^{fl/fl}$ and PIP5KIγ90$^{-/-}$ cells (Figure 9d). Nevertheless, overall tyrosine phosphorylation was slightly elevated in PIP5KIγ90$^{fl/fl}$ compared with PIP5KIγ90$^{-/-}$ cells and in particular FAK Y397 phosphorylation, as an indicator of FAK activity, was more pronounced in PIP5KIγ90$^{fl/fl}$ cells within 90 min of adhesion to fibronectin (Figure 9d). These findings suggest that the local generation of PI-4,5-P_2 by PIP5KIγ90 is critical for maximal activation of FAK, both in response to fibronectin-binding bacteria as well as during cell adhesion to a fibronectin matrix. Therefore, the reduced activation of FAK in the absence of the PIP5KIγ90 isoform can help to explain the impairment in the integrin-mediated internalization of *S. aureus*.

3 | DISCUSSION

Although phosphoinositides make up only a small portion of the lipids present within membranes, they are critical for several cellular processes via regulating local recruitment and activation of PIP-binding proteins. Here we demonstrate that PI-4,5-P_2 is enriched at the sites, where host cell integrins are engaged by *S. aureus* via its fibronectin-binding adhesin FnBP. FnBP-mediated contact is sufficient to trigger increased PI-4,5-P_2 levels, which is due to the local recruitment of the 90 kDa isoform of PIP5KIγ. Murine fibroblasts lacking PIP5KIγ90 are impaired in the integrin-mediated uptake of bacteria suggesting a positive contribution of local PI-4,5-P_2 generation to internalization of *S. aureus*. Indeed, known signaling enzymes downstream of integrin engagement, in particular the focal adhesion kinase, show reduced tyrosine phosphorylation upon bacterial infection of PIP5KIγ90-deficient cells. As the presence and activity of FAK are required for *S. aureus* internalization (Agerer et al., 2005), diminished FAK activity in PIP5KIγ90$^{-/-}$ cells can explain the observed phenotype.

It is well established that PI-4,5-P_2 generated by type I PIP5K at the plasma membrane is a critical regulator of constitutive endocytosis (Posor et al., 2015). In particular, the recruitment and functionality of the clathrin adaptor complex AP2 depend on the interaction of AP2 subunits with PIP5K and PI-4,5-P_2 (Padron et al., 2003). Moreover, increased PI-4,5-P_2 levels at the plasma membrane upon overexpression of PIP5K is important for tubule formation during clathrin-independent and dynamin-dependent endocytosis (Soriano-Castell et al., 2017). In the case of vesicular stomatitis virus (VSV), a virus internalized via clathrin-mediated endocytosis, depletion of PI-4,5-P_2 interferes with viral internalization (Vazquez-Calvo et al., 2012). PIP5KIα appears to be the major PIP5KI family member providing PI-4,5-P_2 during clathrin-mediated endocytosis (Antonescu et al., 2011), whereas PIP5KIγ seems to contribute to clathrin-mediated endocytosis in specific cell types only. Indeed, previous studies have shown that specific ablation of the PIP5KIγ90 isoform in nonneuronal cell types, including murine fibroblasts, does not interfere with clathrin-mediated endocytosis of different plasma membrane receptors (Legate et al., 2011). These findings suggest that PIP5KIα and the remaining PIP5KIγ isoforms are sufficient to allow regular levels of endocytosis in PIP5KIγ90$^{-/-}$ cells and point

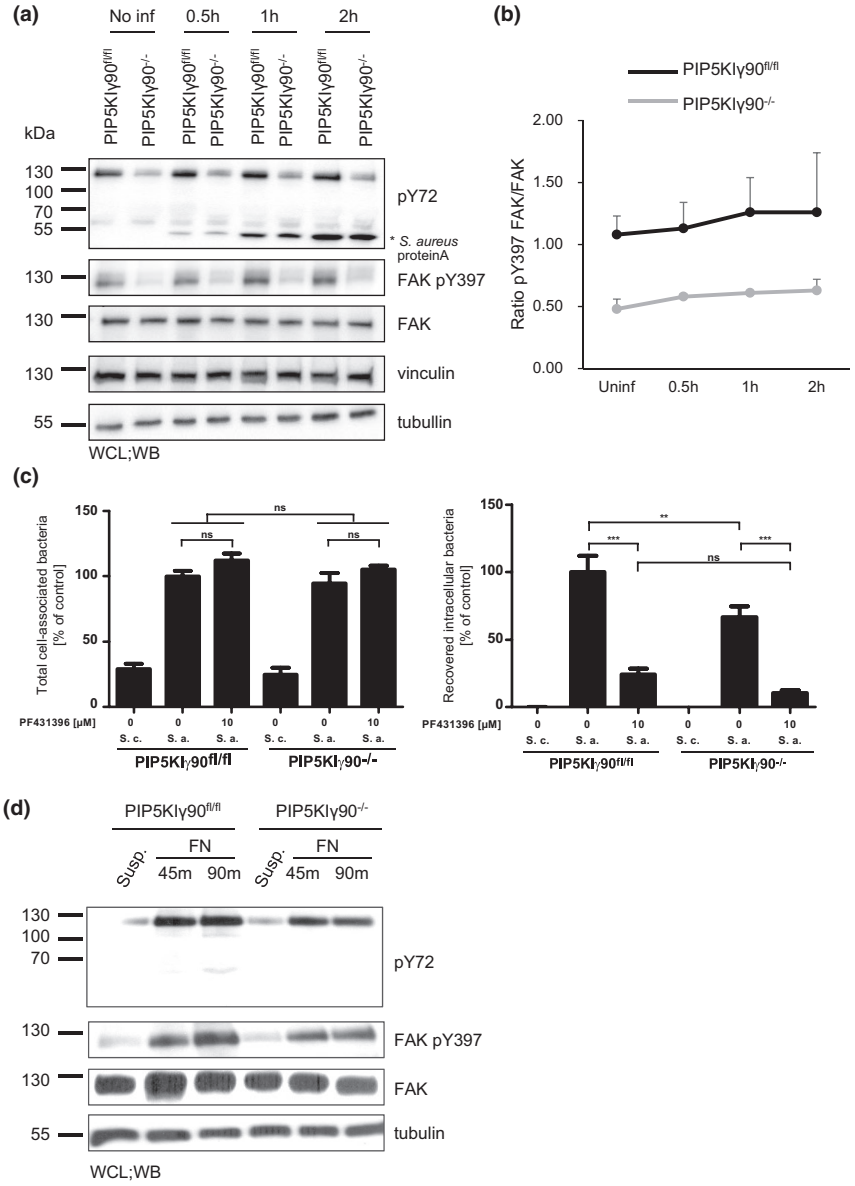

FIGURE 9 PIP5KIγ90 is critical for maximal FAK activation in response to integrin stimulation. (a) PIP5KIγ90$^{fl/fl}$ and PIP5KIγ90$^{-/-}$ cells were serum-starved overnight and then incubated in a suspension medium for 45 min. 1.5 × 10^6 cells were seeded on poly-L-lysine-coated 6 cm dishes and incubated for 1 hr. Then the cells were infected with fibronectin-coated *Staphylococcus aureus* at MOI 100. At indicated time points, whole-cell lysates (WCL) were prepared. WCLs were analyzed by Western blotting with monoclonal pan-phosphotyrosine antibodies (upper panel), a polyclonal phospho-specific antibody recognizing the phosphoY397 (pY397) form of FAK (second panel), a polyclonal rabbit anti-FAK antibody recognizing total FAK (third panel), a monoclonal antibody against vinculin (fourth panel), or a monoclonal antibody against tubulin (lowest panel). The signal derived from *S. aureus* protein A, which binds the secondary antibody and which increases over time due to bacterial growth, is indicated by (*). (b) Signals obtained from two independent experiments as in (a) were analyzed by densitometry and the intensity ratio of p397FAK versus total FAK at different time points is plotted. (c) Cells were seeded and infected as in (a) with *S. aureus* or *S. carnosus* at an MOI = 20 for 2 hr in a growth medium in the presence of 10-μM FAK inhibitor PF431396 or DMSO. The total cell-associated and recovered intracellular bacteria were quantified by gentamicin protection assays. The bars show the mean ± *SEM* of three independent experiments. Values were normalized to PIP5KIγ90$^{fl/fl}$ cells infected with *S. aureus* (control). Significance was evaluated by one-way ANOVA followed by Bonferroni post hoc test. ***$p < .001$. (d) Cells as in (a) were kept in suspension (susp.) or seeded onto fibronectin (15 μg/ml)-coated 6 cm dishes (1.5 × 10^6 cells/dish) for the indicated times. WCLs were analyzed by Western blotting with antibodies as indicated in (a)

to other functions of PIP5KIγ90, which might relate to the integrin-mediated uptake of *S. aureus*.

Besides regulating endocytosis, PI-4,5-P_2 is an important stimulator of actin cytoskeleton dynamics (Mandal, 2020; Saarikangas et al., 2010). At focal adhesion sites, several integrin- and actin-associated proteins have PI-4,5-P_2-binding capability and help to connect integrins to the actomyosin cytoskeleton. More precisely, the integrin-associated proteins talin, kindlin, vinculin, FAK, as well

as α-actinin belong to the core focal adhesion proteins, which are responsive to increased PI-4,5-P_2 levels (Janmey, 1994; Janmey et al., 2018; Kelley et al., 2020; Toker, 2002). In this regard, it has been demonstrated that focal adhesion recruitment of talin and vinculin, but not kindlin, is affected in PIP5KIγ90-deficient cells (Legate et al., 2011). As vinculin is not involved in the uptake of *S. aureus* (Borisova et al., 2013), a reduced integrin-association of talin, due to the absence of PIP5KIγ90, might contribute to a diminished internalization of bacteria. PI-4,5-P_2 binding to the talin head domain is required to release intramolecular inhibitory constraints from this ~280 kDa protein and to allow proper orientation of talin at the inner leaflet of the plasma membrane (Dedden et al., 2019; Elliott et al., 2010; Goksoy et al., 2008; Goult et al., 2013). As a consequence, the recruitment and the spatial orientation of talin at integrin-rich focal adhesion sites are impaired in PIP5KIγ90$^{-/-}$ cells, resulting in slower incorporation of talin into new focal adhesion sites (Legate et al., 2011). Indeed, our results demonstrate that PI-4,5-P_2 production by PIP5KIγ90 is critical to mobilize talin to newly formed integrin clusters beneath fibronectin-bound bacteria.

In the case of *Bartonella henselae*, a Gram-negative, facultative intracellular bacterial pathogen, integrins, and integrin-associated proteins including talin and FAK are required during host cell invasion (Truttmann et al., 2011). *B. henselae* binds endothelial cells and injects into them a panel of bacterial effector proteins to induce a peculiar F-actin-based structure, the so-called invasome (Dehio et al., 1997). While *B. henselae* does not seem to bind integrins, integrin β1 is nevertheless essential for invasome formation, which in turn mediates the engulfment of the bacteria. Interestingly, in this context, talin is important for integrin activation via inside-out-signaling, which is a prerequisite to allow *B. henselae*-induced formation of invasomes (Truttmann et al., 2011). This is in line with the known function of talin during integrin activation, as the talin head domain associates with an NPxY motif in the cytoplasmic tail of integrin β subunits (Calderwood et al., 1999; Tadokoro et al., 2003). Talin binding separates the intracellular domains of the integrin α and β subunits. Thereby, talin triggers the active, extended conformation of the extracellular domains, which allows ligand binding (Shattil et al., 2010). Though talin might be involved in integrin inside-out signaling during *B. henselae* uptake, integrin activation in response to cell-matrix adhesion does not seem to be compromised in PIP5KIγ90-deficient cells (Legate et al., 2011). Furthermore, we do not observe an altered binding of fibronectin-coated *S. aureus* to PIP5KIγ90$^{-/-}$ murine fibroblasts suggesting that talin-mediated inside-out activation of integrins is not critical for this process or that such a process does not depend on PI-4,5-P_2 generated by the PIP5KIγ90 isoform.

Interestingly, recent findings have highlighted the role of PI-4,5-P_2 during activation of the cytoplasmic protein tyrosine kinase FAK (Feng & Mertz, 2015; Goni et al., 2014; Zhou et al., 2015). Similar to talin, FAK harbors an amino-terminal FERM domain, which interacts via basic amino acid residues with acid membrane phospholipids, in particular PI-4,5-P_2. In the absence of PI-4,5-P_2, the FAK FERM domain binds in *cis* to the FAK kinase domain as part of an intramolecular autoinhibition mechanism. Once FAK is recruited to ligand-bound integrins, the local presence of PI-4,5-P_2 can lead to a reorientation of the FERM domain, thereby releasing the inhibitory *cis*-interaction with the kinase domain (Goni et al., 2014; Herzog et al., 2017; Zhou et al., 2015). As a result, FAK enzyme activity, including autophosphorylation of a critical tyrosine residue (FAK Y397) located between the FERM and the kinase domain, initiates a series of further tyrosine phosphorylation events (Sulzmaier et al., 2014). Our observation of reduced FAK tyrosine phosphorylation, and in particular diminished phosphorylation of FAK Y397, in PIP5KIγ90$^{-/-}$ murine fibroblasts upon *S. aureus* infection or upon cell adhesion to fibronectin indicates that this lipid kinase isoform is critical for maximal FAK activity downstream of integrin $\alpha_5\beta_1$. Interestingly, FAK has been shown to contribute to increased PIP5KIγ90 tyrosine phosphorylation, which in turn further reinforces the recruitment of PIP5KIγ90 to integrin-initiated focal adhesion sites (Kong et al., 2006; Ling et al., 2003). Together with our findings, these previous results suggest the existence of a positive feedback loop involving local production of PI-4,5-P_2 by PIP5KIγ90 in response to integrin engagement, recruitment, and full activation of FAK, which then could stimulate further enrichment of PIP5KIγ90 at these sites (Figure S6). Thereby, *S. aureus* hijacks an existing cellular machinery to convert integrins, adhesion receptors specialized in forming mechanically resilient connections to extracellular matrix proteins, into efficient endocytotic devices.

4 | EXPERIMENTAL PROCEDURES

4.1 | Bacteria

Escherichia coli Nova Blue was cultured in Lysogeny Broth (LB) medium at 37°C. *S. aureus* Cowan and nonpathogenic *S. carnosus* TM300 were cultured in Tryptic Soybean Broth medium (TSB; BD Biosciences, Heidelberg, Germany) at 37°C. For the infection, *S. aureus* and *S. carnosus* were grown to reach exponential growth phase, washed twice with PBS, and used to infect cells at a multiplicity of infection (MOI) 20 for gentamicin protection assay or MOI 30 for microscopic evaluation of extra- and intracellular bacterial staining. A GST-FnBP fusion protein was produced and purified from *E. coli* as described (Hoffmann et al., 2010).

4.2 | Cell culture

Human embryonic kidney 293T cells (293 cells) were cultured in DMEM supplemented with 10% calf serum (CS) at 37°C in 5% CO_2. Hela cells were cultured in DMEM with 10% FCS. MEFs from PIP5KIγ90 knockout mouse embryos (PIP5KIγ90$^{-/-}$ cells) and control PIP5KIγ mouse embryos (PIP5KIγ90$^{fl/fl}$ cells) were isolated and immortalized as described (Legate et al., 2011). MEFs were cultured in DMEM with 10% fetal calf serum (FCS) supplemented with non-essential amino acids and sodium pyruvate on gelatine-coated (0.1%

gelatine in PBS) cell culture dishes. All cell lines were subcultured every 2–3 days and were regularly checked for the absence of mycoplasma.

4.3 | DNA constructs and cell transfection

Expression constructs encoding PLCδ-PH–GFP, Akt-PH–GFP, Btk-PH–GFP, and GFP-OSBP-PH were kindly provided by Tamás Balla (NIH, Bethesda, MD), pRKGFP-Talin was kindly provided by Reinhard Fässler. The pDNR-Dual-myrINPP5J construct was generated by PCR amplification using pCMV-SPORT6-hPIPP (clone IRAKp961K1378Q2 from RZPD, Berlin, Germany) as template and primers 5′-GAAGTTATCAGTCGACATGGGATGTATAAAATCAAAA GGGAAAGACAGCGCGGA GCAGCGCAAAGACAA-3′ and anti-5′-TAGAAAGCTTCCGTCCCTGAAGGCAAACTG-3′. The resulting PCR fragment was cloned into pDNR-Dual via SalI/HindIII sites and recombinant vector was transferred into pLPS-3′GFP (Clontech) and pLPS-3′Cerulean by Cre-mediated recombination to generate pLPS-3′myrINPP5J-GFP and pLPS-3′myrINPP5J-Cerulean. The enzymatic inactive INPP5J D153A (myrINPP5J-ia) construct was generated by site-directed mutagenesis using the pDNR-Dual-myrINPP5J as a template and primers sense 5′-GGAATACACAGTCAGCGCTCACAAGCC TGTGGC-3′ and anti-5′-GCCACAGGCTTGTGAGCGCTGACTGTGT ATTCC-3′, then was transferred by Cre-mediated recombination into pLPS-3′GFP and pLPS-3′Cerulean to generate pLPS-3′myrINPP5J-ia-GFP and pLPS-3′myrINPP5J-ia-Cerulean. pEGFP-C1-hPIP5KIγ90 has been described previously (Legate et al., 2011). The hPIP5KIγ90 D253A mutant was generated by site-directed mutagenesis using primers sense 5′-GTTCGCCCTCAAGGGCTCCACCTACAAGAGGCG AGCCAGCAAG-3′ and anti-5′- GGCTCGCCGCTTGTAGGTGGAGCC CTTGAGGGCGAACTTGAGGTG-3′. The pcDNA3.1-mKate-CAAX construct was generated by PCR amplification using pLPS-3′mKate as a template and primers 5′-CTCGGATCCGCCATGGTGTCTAAGGG CG-3′ and anti-5′-GCCTCGAGTTACATCACCACGCAGGGGAGGCC CATGCAGCCCTGATTAAGT TTGTGCCCCAG-3′. The resulting PCR fragment was cloned into pcDNA3.1 via BamHI/XhoI sites.

For the transfection of 293 cells, standard calcium phosphate co-precipitation with 1–5 μg of plasmid DNA for each 10 cm culture dish was used. Fibroblasts were transfected using Lipofectamine 2000 reagent (Invitrogen, Carlsbad, CA) according to the manufacturer's instructions. Cells were employed in infection experiments 24–48 hr after transfection.

4.4 | Genotyping PCR

Genomic DNA was isolated from PIP5KIγ90$^{-/-}$ and control MEF cells using Genomic DNA Mini Kit (Invitrogen) and then was used as a template to perform PCR. Primers used in this experiment were sense 5′-TACTAACTGCTTCCCGCTGCTGC-3′ and anti-5′-GTTTTCTGTGTCTTGTCGTC-3′.

4.5 | Gentamicin protection assay

2×10^5 293 cells or 5×10^4 MEFs were seeded into poly-L-lysine-coated 24-well plates. Cells were infected at MOI 20 for 2 hr at 37°C and 5% CO_2. To evaluate the number of intracellular bacteria, the medium was carefully replaced with a fresh medium containing 50 μg/ml gentamicin. After incubation for 1 hr at 37°C, intracellular bacteria were released by treatment with 0.5% saponin for 15 min at 37°C. Released bacteria were diluted in PBS and plated on TSB agar plates to determine the colony-forming units (cfu), which resemble the "Recovered intracellular bacteria." In parallel samples, infected cells were gently washed with PBS, lysed with 0.5% saponin without prior gentamicin treatment and dilutions were plated on TSB agar plates. In that way, the "total cell-associated bacteria" were enumerated.

4.6 | Extra- and intracellular bacteria staining and fluorescence microscopy examination

For PIP5KIγ90$^{-/-}$ and control MEF cells, 3×10^4 cells for each cell line were seeded on poly-L-lysine-coated, acid-washed glass coverslips in a 24-well plate. The next day, cells were infected with *S. aureus* at MOI 30 for 2 hr, then washed twice with PBS$^{+/+}$ (1× PBS containing $CaCl_2$ and $MgCl_2$) and fixed with 4% paraformaldehyde (PFA) for 20 min at RT. After this, cells were incubated in a blocking buffer (PBS$^{+/+}$ plus 10% FCS) for 10 min. Extracellular bacteria were detected by rabbit polyclonal α-staphylococcal serum diluted in blocking buffer (45 min at RT). Afterward, samples were washed three times with PBS$^{+/+}$ and incubated with goat α-rabbit IgG-Cy5 (Jackson Immunoresearch) in the dark for 30 min. Then, cells were washed three times and permeabilized by 0.5% Triton/PBS. Ten minutes later, cells were washed three times with PBS$^{+/+}$, blocked for 10 min, and incubated with rabbit polyclonal α-staphylococcal serum at RT. Forty-five minutes later, samples were washed three times with PBS$^{+/+}$ and incubated with goat α-rabbit IgG coupled to Cy2 in the dark for 30 min. Finally, after three washes with PBS$^{+/+}$, the coverslips were embedded in mounting medium (DaKo, Glostrup, Denmark) on glass slides and sealed with nail polish. Images were acquired with a Leica AF6000LX fluorescence microscope and processed with ImageJ.

For the experiment performed in 293 cells, 2×10^5 transfected cells were seeded on poly-L-lysine-coated glass coverslips in a 24-well plate. Two hours later, cells were infected with pacific-blue stained and biotin-labeled *S. aureus* at MOI 30 for 2 hr, then washed twice with PBS$^{+/+}$ and fixed with 4% PFA for 20 min at RT. After this, cells were incubated in a blocking buffer solution for 10 min. Afterward, cells were incubated with streptavidin-AlexaFluor647 for 1 hr at RT in the dark. Finally, after three washes with PBS$^{+/+}$, the coverslips were transferred to glass slides, embedded in mounting medium, and sealed with nail polish. Images were acquired with a Leica AF6000LX fluorescence microscope.

For immunofluorescence staining of transfected PIP5KIγ90$^{-/-}$ cells, 5×10^4 cells were seeded on poly-L-lysine-coated coverslips in a 24-well plate. The next day, cells were transfected with indicated plasmid DNA. Twenty-four hours after transfection, cells were infected with pacific-blue stained and biotin-labeled *S. aureus* at MOI 30 for 2 hr. After the infection, the same staining and measuring procedure as described above for the transfected 293 cells were used.

For cell membrane staining, cells were fixed with 4% PFA, washed three times in PBS and incubated for 10 min in blocking buffer. Cells were stained with CellMask Orange Plasma membrane stain (Invitrogen, cat. No.: C10045) diluted in blocking buffer at a final concentration of 5 μg/ml for 10 min.

4.7 | Live cell imaging

Cells were seeded into poly-L-lysine-coated 3.5 cm dishes (with integrated coverslip), for example, 5×10^4 cells/dish. The next day, exchange of DMEM medium with colorless DMEM and preparation of the CLSM (heating of incubation chamber to 37°C and connection of CO_2 supply) followed. If the bacterial infection was investigated, cells were directly infected with the fluorescence-stained *S. aureus* at MOI 60. First of all, appropriate cells were searched (e.g., the transfected cells). Then the settings were adjusted and finally, the movie was started to record. The interval in this study was 3 min. Images and movies were analyzed by LAS software and Image J.

4.8 | Quantification of surface integrin expression by flow cytometry

Integrin α_5 (clone 5H10-27(MFR5)) and integrin α_V (clone RMV-7) antibodies were purchased from BD Biosciences. Integrin β_1 (clone HMβ1-1) was obtained from Biolegend and integrin β_3 antibody (clone HMb3-1) from Millipore (MA, US). Secondary antibodies (biotin-SP-conjugated goat α-rat IgG), streptavidin-FITC, and Rhodamine Red-X-AffiniPure Goat Anti-Armenian Hamster IgG (H+L) were purchased from Jackson ImmunoResearch (West Grove, PA). For quantification of surface integrin expression, suspended fibroblasts were incubated in suspension medium (DMEM containing 0.25% BSA) for 40 min at 37°C. Then, 2×10^5 cells were incubated with appropriate primary antibodies (diluted 1:300) in FACS buffer (5% heat-inactivated FCS, 1% sodium azide in PBS) for 1 hr at 4°C. After washing, secondary antibodies were applied for 1 hr at 4°C, then washed again, samples were analyzed by flow cytometry (LSRII, BD Biosciences).

4.9 | Small interfering RNA transfection

To obtain siRNA-mediated knockdown of PIP5 kinases, Hela cells instead of 293 cells were used. The siRNA oligonucleotides against PIP5KIα, PIP5KIβ, and PIP5KIγ were purchased from Thermo Scientific. The siRNA transfection was performed according to the manufacturer's instructions. Forty-eight hours after transfection, total RNA was isolated using RNeasy Mini Kit (Qiagen, Hilden, Germany) and further used for the quantitative real-time PCR to evaluate the mRNA levels of PIP5KI.

4.10 | qRT-PCR evaluation of PIP5K mRNA levels

Isolation of total RNA from HeLa cells was performed using RNeasy Mini Kit (Qiagen, Hilden, Germany). About 1–2 μg of total RNA was applied for the reverse transcription. Quantitative real-time PCR was conducted with the sensiMixPlus SYBR Kit (Quantace, Germany) with the following cycle conditions: 95°C for 10 min followed by 40 cycles at 95°C for 10 s, 60°C for 20 s, and 72°C for 20 s. Relative expression of PIP5KIα, β, pan-γ, or γ90 was normalized by glyceraldehyde-3-phosphate dehydrogenase (GAPDH) according to Livak and Schmittgen (2001). The primers used were: hPIP5Kiα (forward: 5′-GCGTGATGTCCTCATGCAAG-3′; reverse: 5′-GAAGTAGCGGAAGGCAACAG-3′), hPIP5KIβ (forward: 5′-TAGCCAGGAATGGAAGGATG-3′; reverse: 5′-CCAAGGAAGCAG CTTCAAAC-3′), hPIP5KIγ (forward: 5′-CGTGCAGCGTGGAGATTGT G-3′; reverse: 5′-GCCTGGCTGGCAGTTTCTAC-3′), hGAPDH (forward: 5′-GAAGGTGAAGGTCGGAGTCA-3′; reverse: 5′-TTGAGGTC AATGAAGGGGTC-3′).

4.11 | Cell lysis and western blotting

Cell lysis and western blotting were performed as described (Schmitter et al., 2004) with some modifications. Briefly, protein concentration was assessed using Pierce bicinchoninic assay kit (Thermo Fisher Scientific, Waltham, MA). Equal amounts of proteins were loaded on SDS-PAGE gels. Monoclonal antibody against GFP (clone JL-8) was purchased from Clontech and against vinculin (clone hVIN1) was from Sigma-Aldrich. Antibody against β-tubulin (clone E-7, DSHB, University of Iowa) was purified from hybridoma cell supernatants. Polyclonal rabbit antibodies against integrin β1 (M-106), Cortactin (H-191), and FAK (A-17) were from Santa Cruz Biotechnology. Antibody against FAK pY397 was purchased from Biosource, phosphotyrosine (pY72) monoclonal antibody was purchased from Covance (USA). Goat-antimouse and goat-antirabbit IgG coupled to HRP were purchased from Jackson ImmunoResearch.

4.12 | Fluorescence intensity profile

The corresponding images were digitally processed with Image J (Wayne Rasband, National Institutes of Health, USA) and merged to yield pseudo-colored RGB pictures. The fluorescence intensity at bacterial attachment sites was measured and normalized by the maximal value gained from bacteria staining. The fluorescence percentage was calculated by Graphpad prism 5.

4.13 | Statistics

Infection and flow cytometry experiments were performed at least three times, and data were presented as mean ± *SEM*. Differences in adherence and internalization of *S. aureus* were analyzed by unpaired Student's *t* test. In all analyses, a *p* value of <.05 was considered to be statistically significant.

ACKNOWLEDGMENTS

We are indebted to S. Feindler-Boeckh for excellent technical support, Tamás Balla (NIH, Bethesda, MD) for providing GFP-PH domain constructs, and Benedikt Podhorny for initial analyses with PH domains. Y.S. is recipient of a fellowship from the Chinese Scholarship Council (CSC) and an associate fellow of the Graduate School Biological Sciences at the University of Konstanz. This work was supported by DFG Priority Program SPP1150 grant Ha 2856/5-1 to C.R.H. Open Access funding enabled and organized by Projekt DEAL.

CONFLICT OF INTEREST

The authors declare that they have no competing interests.

ORCID

Christof R. Hauck https://orcid.org/0000-0002-1005-2141

REFERENCES

Agerer, F., Lux, S., Michel, A., Rohde, M., Ohlsen, K. & Hauck, C.R. (2005) Cellular invasion by *Staphylococcus aureus* reveals a functional link between focal adhesion kinase and cortactin in integrin-mediated internalisation. *Journal of Cell Science*, *118*, 2189–2200.

Agerer, F., Michel, A., Ohlsen, K. & Hauck, C.R. (2003) Integrin-mediated invasion of *Staphylococcus aureus* into human cells requires Src family protein tyrosine kinases. *Journal of Biological Chemistry*, *278*, 42524–42531. https://doi.org/10.1074/jbc.M302096200

Antonescu, C.N., Aguet, F., Danuser, G. & Schmid, S.L. (2011) Phosphatidylinositol-(4,5)-bisphosphate regulates clathrin-coated pit initiation, stabilization, and size. *Molecular Biology of the Cell*, *22*, 2588–2600. https://doi.org/10.1091/mbc.e11-04-0362

Arciola, C.R., Campoccia, D. & Montanaro, L. (2018) Implant infections: adhesion, biofilm formation and immune evasion. *Nature Reviews Microbiology*, *16*, 397–409. https://doi.org/10.1038/s41579-018-0019-y

Balla, T. (2005) Inositol-lipid binding motifs: signal integrators through protein-lipid and protein-protein interactions. *Journal of Cell Science*, *118*, 2093–2104. https://doi.org/10.1242/jcs.02387

Balla, T. & Varnai, P. (2009) Visualization of cellular phosphoinositide pools with GFP-fused protein-domains. *Current Protocols in Cell Biology/Editorial Board Juan S Bonifacino [et al]*, Chapter 24, Unit 24.4. https://doi.org/10.1002/0471143030.cb2404s42

Borisova, M., Shi, Y., Buntru, A., Wörner, S., Ziegler, W.H. & Hauck, C.R. (2013) Integrin-mediated internalization of *Staphylococcus aureus* does not require vinculin. *BMC Cell Biology*, *14*, 2. https://doi.org/10.1186/1471-2121-14-2

Brouillette, E., Talbot, B.G. & Malouin, F. (2003) The fibronectin-binding proteins of *Staphylococcus aureus* may promote mammary gland colonization in a lactating mouse model of mastitis. *Infection and Immunity*, *71*, 2292–2295.

Calderwood, D.A., Zent, R., Grant, R., Rees, D.J., Hynes, R.O. & Ginsberg, M.H. (1999) The talin head domain binds to integrin beta subunit cytoplasmic tails and regulates integrin activation. *Journal of Biological Chemistry*, *274*, 28071–28074.

Chinthalapudi, K., Rangarajan, E.S. & Izard, T. (2018) The interaction of talin with the cell membrane is essential for integrin activation and focal adhesion formation. *Proceedings of the National Academy of Sciences of the United States of America*, *115*, 10339–10344. https://doi.org/10.1073/pnas.1806275115

Daste, F., Walrant, A., Holst, M.R., Gadsby, J.R., Mason, J., Lee, J.-E. et al. (2017) Control of actin polymerization via the coincidence of phosphoinositides and high membrane curvature. *Journal of Cell Biology*, *216*, 3745–3765. https://doi.org/10.1083/jcb.201704061

Dautry-Varsat, A., Subtil, A. & Hackstadt, T. (2005) Recent insights into the mechanisms of *Chlamydia* entry. *Cellular Microbiology*, *7*, 1714–1722. https://doi.org/10.1111/j.1462-5822.2005.00627.x

Dedden, D., Schumacher, S., Kelley, C.F., Zacharias, M., Biertumpfel, C., Fassler, R. et al. (2019) The architecture of talin1 reveals an autoinhibition mechanism. *Cell*, *179*, 120–131.e13. https://doi.org/10.1016/j.cell.2019.08.034

Dehio, C., Meyer, M., Berger, J., Schwarz, H. & Lanz, C. (1997) Interaction of *Bartonella henselae* with endothelial cells results in bacterial aggregation on the cell surface and the subsequent engulfment and internalisation of the bacterial aggregate by a unique structure, the invasome. *Journal of Cell Science*, *110*(Pt 18), 2141–2154.

Di Paolo, G. & De Camilli, P. (2006) Phosphoinositides in cell regulation and membrane dynamics. *Nature*, *443*, 651–657. https://doi.org/10.1038/nature05185

Di Paolo, G., Pellegrini, L., Letinic, K., Cestra, G., Zoncu, R., Voronov, S. et al. (2002) Recruitment and regulation of phosphatidylinositol phosphate kinase type 1 gamma by the FERM domain of talin. *Nature*, *420*, 85–89.

Doughman, R.L., Firestone, A.J., Wojtasiak, M.L., Bunce, M.W. & Anderson, R.A. (2003) Membrane ruffling requires coordination between type Ialpha phosphatidylinositol phosphate kinase and Rac signaling. *Journal of Biological Chemistry*, *278*, 23036–23045.

Durand, N., Bastea, L.I., Long, J., Doppler, H., Ling, K. & Storz, P. (2016) Protein Kinase D1 regulates focal adhesion dynamics and cell adhesion through phosphatidylinositol-4-phosphate 5-kinase type-I gamma. *Scientific Reports*, *6*, 35963.

Dziewanowska, K., Patti, J.M., Deobald, C.F., Bayles, K.W., Trumble, W.R. & Bohach, G.A. (1999) Fibronectin binding protein and host cell tyrosine kinase are required for internalization of *Staphylococcus aureus* by epithelial cells. *Infection and Immunity*, *67*, 4673–4678.

Elliott, P.R., Goult, B.T., Kopp, P.M., Bate, N., Grossmann, J.G., Roberts, G.C. et al. (2010) The Structure of the talin head reveals a novel extended conformation of the FERM domain. *Structure*, *18*, 1289–1299.

Feng, J. & Mertz, B. (2015) Novel phosphotidylinositol 4,5-bisphosphate binding sites on focal adhesion kinase. *PLoS One*, *10*, e0132833. https://doi.org/10.1371/journal.pone.0132833

Foster, T.J. (2016) The remarkably multifunctional fibronectin binding proteins of *Staphylococcus aureus*. *European Journal of Clinical Microbiology and Infectious Diseases*, *35*, 1923–1931. https://doi.org/10.1007/s10096-016-2763-0

Foster, T.J., Geoghegan, J.A., Ganesh, V.K. & Hook, M. (2014) Adhesion, invasion and evasion: the many functions of the surface proteins of *Staphylococcus aureus*. *Nature Reviews Microbiology*, *12*, 49–62. https://doi.org/10.1038/nrmicro3161

Fowler, T., Johansson, S., Wary, K.K. & Hook, M. (2003) Src kinase has a central role in in vitro cellular internalization of *Staphylococcus aureus*. *Cellular Microbiology*, *5*, 417–426. https://doi.org/10.1046/j.1462-5822.2003.00290.x

Goksoy, E., Ma, Y.Q., Wang, X., Kong, X., Perera, D., Plow, E.F. et al. (2008) Structural basis for the autoinhibition of talin in regulating integrin activation. *Molecular Cell*, *31*, 124–133. https://doi.org/10.1016/j.molcel.2008.06.011

Goni, G.M., Epifano, C., Boskovic, J., Camacho-Artacho, M., Zhou, J., Bronowska, A. et al. (2014) Phosphatidylinositol 4,5-bisphosphate

triggers activation of focal adhesion kinase by inducing clustering and conformational changes. *Proceedings of the National Academy of Sciences of the United States of America*, *111*, E3177–E3186. https://doi.org/10.1073/pnas.1317022111

Goult, B.T., Xu, X.-P., Gingras, A.R., Swift, M., Patel, B., Bate, N. et al. (2013) Structural studies on full-length talin1 reveal a compact auto-inhibited dimer: implications for talin activation. *Journal of Structural Biology*, *184*, 21–32. https://doi.org/10.1016/j.jsb.2013.05.014

Hauck, C.R., Borisova, M. & Muenzner, P. (2012) Exploitation of integrin function by pathoghenic microbes. *Current Opinion Cell Biology*, *24*, 637–644.

Henderson, B., Nair, S., Pallas, J. & Williams, M.A. (2011) Fibronectin: a multidomain host adhesin targeted by bacterial fibronectin-binding proteins. *FEMS Microbiology Reviews*, *35*, 147–200. https://doi.org/10.1111/j.1574-6976.2010.00243.x

Herzog, F.A., Braun, L., Schoen, I. & Vogel, V. (2017) Structural insights how PIP2 imposes preferred binding orientations of FAK at lipid membranes. *The Journal of Physical Chemistry B*, *121*, 3523–3535. https://doi.org/10.1021/acs.jpcb.6b09349

Hoffmann, C., Berking, A., Agerer, F., Buntru, A., Neske, F., Chhatwal, G.S. et al. (2010) Caveolin limits membrane microdomain mobility and integrin-mediated uptake of fibronectin-binding pathogens. *Journal of Cell Science*, *123*, 4280–4291. https://doi.org/10.1242/jcs.064006

Huveneers, S., Truong, H., Fassler, R., Sonnenberg, A. & Danen, E.H. (2008) Binding of soluble fibronectin to integrin alpha5 beta1 - link to focal adhesion redistribution and contractile shape. *Journal of Cell Science*, *121*, 2452–2462.

Hymes, J.P. & Klaenhammer, T.R. (2016) Stuck in the middle: fibronectin-binding proteins in gram-positive bacteria. *Frontiers in Microbiology*, *7*, 1504.

Ishihara, H., Shibasaki, Y., Kizuki, N., Katagiri, H., Yazaki, Y., Asano, T. et al. (1996) Cloning of cDNAs encoding two isoforms of 68-kDa type I phosphatidylinositol-4-phosphate 5-kinase. *Journal of Biological Chemistry*, *271*, 23611–23614. https://doi.org/10.1074/jbc.271.39.23611

Ishihara, H., Shibasaki, Y., Kizuki, N., Wada, T., Yazaki, Y., Asano, T. et al. (1998) Type I phosphatidylinositol-4-phosphate 5-kinases. Cloning of the third isoform and deletion/substitution analysis of members of this novel lipid kinase family. *Journal of Biological Chemistry*, *273*, 8741–8748. https://doi.org/10.1074/jbc.273.15.8741

Janmey, P.A. (1994) Phosphoinositides and calcium as regulators of cellular actin assembly and disassembly. *Annual Review of Physiology*, *56*, 169–191. https://doi.org/10.1146/annurev.ph.56.030194.001125

Janmey, P.A., Bucki, R. & Radhakrishnan, R. (2018) Regulation of actin assembly by PI(4,5)P2 and other inositol phospholipids: an update on possible mechanisms. *Biochemical and Biophysical Research Communications*, *506*, 307–314. https://doi.org/10.1016/j.bbrc.2018.07.155

Jenkins, G.H., Fisette, P.L. & Anderson, R.A. (1994) Type I phosphatidylinositol 4-phosphate 5-kinase isoforms are specifically stimulated by phosphatidic acid. *Journal of Biological Chemistry*, *269*, 11547–11554. https://doi.org/10.1016/S0021-9258(19)78159-9

Kelley, C.F., Litschel, T., Schumacher, S., Dedden, D., Schwille, P. & Mizuno, N. (2020) Phosphoinositides regulate force-independent interactions between talin, vinculin, and actin. *eLife*, *9*, e56110.

Kong, X., Wang, X., Misra, S. & Qin, J. (2006) Structural basis for the phosphorylation-regulated focal adhesion targeting of type Igamma phosphatidylinositol phosphate kinase (PIPKIgamma) by talin. *Journal of Molecular Biology*, *359*, 47–54.

Konkel, M.E., Talukdar, P.K., Negretti, N.M. & Klappenbach, C.M. (2020) Taking control: *Campylobacter jejuni* binding to fibronectin sets the stage for cellular adherence and invasion. *Frontiers in Microbiology*, *11*, 564. https://doi.org/10.3389/fmicb.2020.00564

Kwiatkowska, K. (2010) One lipid, multiple functions: how various pools of PI(4,5)P(2) are created in the plasma membrane. *Cellular and Molecular Life Sciences*, *67*, 3927–3946. https://doi.org/10.1007/s00018-010-0432-5

Legate, K.R., Montag, D., Bottcher, R.T., Takahashi, S. & Fassler, R. (2012) Comparative phenotypic analysis of the two major splice isoforms of phosphatidylinositol phosphate kinase type Igamma in vivo. *Journal of Cell Science*, *125*, 5636–5646.

Legate, K.R., Takahashi, S., Bonakdar, N., Fabry, B., Boettiger, D., Zent, R. et al. (2011) Integrin adhesion and force coupling are independently regulated by localized PtdIns(4,5)(2) synthesis. *The EMBO Journal*, *30*, 4539–4553.

Levine, T.P. & Munro, S. (2002) Targeting of Golgi-specific pleckstrin-homology domains involves both PtdIns 4-kinase-dependent and-independent components. *Current Biology*, *12*, 695–704.

Ling, K., Doughman, R.L., Firestone, A.J., Bunce, M.W. & Anderson, R.A. (2002) Type I gamma phosphatidylinositol phosphate kinase targets and regulates focal adhesions. *Nature*, *420*, 89–93.

Ling, K., Doughman, R.L., Iyer, V.V., Firestone, A.J., Bairstow, S.F., Mosher, D.F. et al. (2003) Tyrosine phosphorylation of type Igamma phosphatidylinositol phosphate kinase by Src regulates an integrin-talin switch. *Journal of Cell Biology*, *163*, 1339–1349.

Liu, C., Bayer, A., Cosgrove, S.E., Daum, R.S., Fridkin, S.K., Gorwitz, R.J. et al. (2011) Clinical practice guidelines by the infectious diseases society of america for the treatment of methicillin-resistant *Staphylococcus aureus* infections in adults and children. *Clinical Infectious Diseases*, *52*, e18–e55. https://doi.org/10.1093/cid/ciq146

Livak, K.J. & Schmittgen, T.D. (2001) Analysis of relative gene expression data using real-time quantitative PCR and the 2(-Delta Delta C(T)) method. *Methods*, *25*, 402–408.

Loijens, J.C. & Anderson, R.A. (1996) Type I phosphatidylinositol-4-phosphate 5-kinases are distinct members of this novel lipid kinase family. *Journal of Biological Chemistry*, *271*, 32937–32943. https://doi.org/10.1074/jbc.271.51.32937

Mandal, K. (2020) Review of PIP2 in cellular signaling, functions and diseases. *International Journal of Molecular Sciences*, *21*, 8342. https://doi.org/10.3390/ijms21218342

Marjenberg, Z.R., Ellis, I.R., Hagan, R.M., Prabhakaran, S., Hook, M., Talay, S.R. et al. (2010) Cooperative binding and activation of fibronectin by a bacterial surface protein. *Journal of Biological Chemistry*, *286*, 1884–1894. https://doi.org/10.1074/jbc.M110.183053

Martin, T.F. (1998) Phosphoinositide lipids as signaling molecules: common themes for signal transduction, cytoskeletal regulation, and membrane trafficking. *Annual Review of Cell and Developmental Biology*, *14*, 231–264. https://doi.org/10.1146/annurev.cellbio.14.1.231

Mayinger, P. (2012) Phosphoinositides and vesicular membrane traffic. *Biochimica et Biophysica Acta (BBA) - Molecular and Cell Biology of Lipids*, *1821*, 1104–1113. https://doi.org/10.1016/j.bbalip.2012.01.002

Nader, G.P., Ezratty, E.J. & Gundersen, G.G. (2016) FAK, talin and PIPKIgamma regulate endocytosed integrin activation to polarize focal adhesion assembly. *Nature Cell Biology*, *18*, 491–503.

Niebuhr, K., Giuriato, S., Pedron, T., Philpott, D.J., Gaits, F., Sable, J. et al. (2002) Conversion of PtdIns(4,5)P(2) into PtdIns(5)P by the *S. flexneri* effector IpgD reorganizes host cell morphology. *The EMBO Journal*, *21*, 5069–5078. https://doi.org/10.1093/emboj/cdf522

Oppelt, A., Lobert, V.H., Haglund, K., Mackey, A.M., Rameh, L.E., Liestøl, K. et al. (2013) Production of phosphatidylinositol 5-phosphate via PIKfyve and MTMR3 regulates cell migration. *EMBO Reports*, *14*, 57–64. https://doi.org/10.1038/embor.2012.183

Padron, D., Wang, Y.J., Yamamoto, M., Yin, H. & Roth, M.G. (2003) Phosphatidylinositol phosphate 5-kinase Ibeta recruits AP-2 to the plasma membrane and regulates rates of constitutive endocytosis. *Journal of Cell Biology*, *162*, 693–701.

Posor, Y., Eichhorn-Grunig, M. & Haucke, V. (2015) Phosphoinositides in endocytosis. *Biochimica et Biophysica Acta Acta (BBA) - Molecular*

and Cell Biology of Lipids, *1851*, 794–804. https://doi.org/10.1016/j.bbalip.2014.09.014

Saarikangas, J., Zhao, H. & Lappalainen, P. (2010) Regulation of the actin cytoskeleton-plasma membrane interplay by phosphoinositides. *Physiological Reviews*, *90*, 259–289. https://doi.org/10.1152/physrev.00036.2009

Sarantis, H., Balkin, D.M., De Camilli, P., Isberg, R.R., Brumell, J.H. & Grinstein, S. (2012) *Yersinia* entry into host cells requires Rab5-dependent dephosphorylation of PI(4,5)P and membrane scission. *Cell Host and Microbe*, *11*, 117–128.

Schmitter, T., Agerer, F., Peterson, L., Muenzner, P. & Hauck, C.R. (2004) Granulocyte CEACAM3 is a phagocytic receptor of the innate immune system that mediates recognition and elimination of human-specific pathogens. *Journal of Experimental Medicine*, *199*, 35–46. https://doi.org/10.1084/jem.20030204

Schroder, A., Schroder, B., Roppenser, B., Linder, S., Sinha, B., Fassler, R. et al. (2006) *Staphylococcus aureus* fibronectin binding protein-A induces motile attachment sites and complex actin remodeling in living endothelial cells. *Molecular Biology of the Cell*, *17*, 5198–5210.

Shattil, S.J., Kim, C. & Ginsberg, M.H. (2010) The final steps of integrin activation: the end game. *Nature Reviews Molecular Cell Biology*, *11*, 288–300. https://doi.org/10.1038/nrm2871

Sieradzki, K., Roberts, R.B., Haber, S.W. & Tomasz, A. (1999) The development of vancomycin resistance in a patient with methicillin-resistant *Staphylococcus aureus* infection. *The New England Journal of Medicine*, *340*, 517–523.

Sinha, B., Francois, P.P., Nusse, O., Foti, M., Hartford, O.M., Vaudaux, P. et al. (1999) Fibronectin-binding protein acts as *Staphylococcus aureus* invasin via fibronectin bridging to integrin alpha5beta1. *Cellular Microbiology*, *1*, 101–117. https://doi.org/10.1046/j.1462-5822.1999.00011.x

Soriano-Castell, D., Chavero, A., Rentero, C., Bosch, M., Vidal-Quadras, M., Pol, A. et al. (2017) ROCK1 is a novel Rac1 effector to regulate tubular endocytic membrane formation during clathrin-independent endocytosis. *Scientific Reports*, *7*, 6866. https://doi.org/10.1038/s41598-017-07130-x

Strohmeyer, N., Bharadwaj, M., Costell, M., Fassler, R. & Muller, D.J. (2017) Fibronectin-bound alpha5beta1 integrins sense load and signal to reinforce adhesion in less than a second. *Nature Materials*, *16*, 1262–1270.

Sulzmaier, F.J., Jean, C. & Schlaepfer, D.D. (2014) FAK in cancer: mechanistic findings and clinical applications. *Nature Reviews Cancer*, *14*, 598–610. https://doi.org/10.1038/nrc3792

Tadokoro, S., Shattil, S.J., Eto, K., Tai, V., Liddington, R.C., de Pereda, J.M. et al. (2003) Talin binding to integrin beta tails: a final common step in integrin activation. *Science*, *302*, 103–106.

Terebiznik, M.R., Vieira, O.V., Marcus, S.L., Slade, A., Yip, C.M., Trimble, W.S. et al. (2002) Elimination of host cell PtdIns(4,5)P(2) by bacterial SigD promotes membrane fission during invasion by *Salmonella*. *Nature Cell Biology*, *4*, 766–773. https://doi.org/10.1038/ncb854

Toker, A. (2002) Phosphoinositides and signal transduction. *Cellular and Molecular Life Sciences*, *59*, 761–779. https://doi.org/10.1007/s00018-002-8465-z

Truttmann, M.C., Misselwitz, B., Huser, S., Hardt, W.D., Critchley, D.R. & Dehio, C. (2011) *Bartonella henselae* engages inside-out and outside-in signaling by integrin beta1 and talin1 during invasome-mediated bacterial uptake. *Journal of Cell Science*, *124*, 3591–3602.

Tsiodras, S., Gold, H.S., Sakoulas, G., Eliopoulos, G.M., Wennersten, C., Venkataraman, L. et al. (2001) Linezolid resistance in a clinical isolate of *Staphylococcus aureus*. *The Lancet*, *358*, 207–208. https://doi.org/10.1016/S0140-6736(01)05410-1

Turner, N.A., Sharma-Kuinkel, B.K., Maskarinec, S.A., Eichenberger, E.M., Shah, P.P., Carugati, M. et al. (2019) Methicillin-resistant *Staphylococcus aureus*: an overview of basic and clinical research. *Nature Reviews Microbiology*, *17*, 203–218. https://doi.org/10.1038/s41579-018-0147-4

Vakonakis, I., Staunton, D., Ellis, I.R., Sarkies, P., Flanagan, A., Schor, A.M. et al. (2009) Motogenic sites in human fibronectin are masked by long range interactions. *Journal of Biological Chemistry*, *284*, 15668–15675. https://doi.org/10.1074/jbc.M109.003673

van den Bout, I. & Divecha, N. (2009) PIP5K-driven PtdIns(4,5)P2 synthesis: regulation and cellular functions. *Journal of Cell Science*, *122*, 3837–3850.

Vazquez-Calvo, A., Sobrino, F. & Martin-Acebes, M.A. (2012) Plasma membrane phosphatidylinositol 4,5 bisphosphate is required for internalization of foot-and-mouth disease virus and vesicular stomatitis virus. *PLoS One*, *7*, e45172. https://doi.org/10.1371/journal.pone.0045172

Vuento, M. & Vaheri, A. (1979) Purification of fibronectin from human plasma by affinity chromatography under non-denaturing conditions. *Biochemical Journal*, *183*, 331–337. https://doi.org/10.1042/bj1830331

Wong, K.W. & Isberg, R.R. (2003) Arf6 and phosphoinositol-4-phosphate-5-kinase activities permit bypass of the Rac1 requirement for beta1 integrin-mediated bacterial uptake. *Journal of Experimental Medicine*, *198*, 603–614.

Zhou, J., Bronowska, A., Le Coq, J., Lietha, D. & Grater, F. (2015) Allosteric regulation of focal adhesion kinase by PIP(2) and ATP. *Biophysical Journal*, *108*, 698–705. https://doi.org/10.1016/j.bpj.2014.11.3454

SUPPORTING INFORMATION

Additional supporting information may be found in the online version of the article at the publisher's website.

How to cite this article: Shi, Y., Berking, A., Baade, T., Legate, K.R., Fässler, R. & Hauck, C.R. (2021) PIP5KIγ90-generated phosphatidylinositol-4,5-bisphosphate promotes the uptake of *Staphylococcus aureus* by host cells. *Molecular Microbiology*, 116, 1249–1267. https://doi.org/10.1111/mmi.14807